



# Cytoplasmic Polyadenylation Is an Ancestral Hallmark of Early Development in Animals

Labib Rouhana <sup>\*</sup>,<sup>1</sup> Allison Edgar,<sup>2</sup> Fredrik Hugosson,<sup>2</sup> Valeria Dountcheva,<sup>1</sup> Mark Q. Martindale,<sup>2,3</sup> and Joseph F. Ryan <sup>2,3</sup>

<sup>1</sup>Department of Biology, University of Massachusetts Boston, Boston, MA, USA

<sup>2</sup>Whitney Laboratory for Marine Bioscience, University of Florida, St. Augustine, FL, USA

<sup>3</sup>Department of Biology, University of Florida, Gainesville, FL, USA

\*Corresponding author: E-mail: labib.rouhana@umb.edu.

Associate editor: Dr. Jian Lu

## Abstract

Differential regulation of gene expression has produced the astonishing diversity of life on Earth. Understanding the origin and evolution of mechanistic innovations for control of gene expression is therefore integral to evolutionary and developmental biology. Cytoplasmic polyadenylation is the biochemical extension of polyadenosine at the 3'-end of cytoplasmic mRNAs. This process regulates the translation of specific maternal transcripts and is mediated by the Cytoplasmic Polyadenylation Element-Binding Protein family (CPEBs). Genes that code for CPEBs are amongst a very few that are present in animals but missing in nonanimal lineages. Whether cytoplasmic polyadenylation is present in non-bilaterian animals (i.e., sponges, ctenophores, placozoans, and cnidarians) remains unknown. We have conducted phylogenetic analyses of CPEBs, and our results show that CPEB1 and CPEB2 subfamilies originated in the animal stem lineage. Our assessment of expression in the sea anemone, *Nematostella vectensis* (Cnidaria), and the comb jelly, *Mnemiopsis leidyi* (Ctenophora), demonstrates that maternal expression of CPEB1 and the catalytic subunit of the cytoplasmic polyadenylation machinery (GLD2) is an ancient feature that is conserved across animals. Furthermore, our measurements of poly(A)-tail elongation reveal that key targets of cytoplasmic polyadenylation are shared between vertebrates, cnidarians, and ctenophores, indicating that this mechanism orchestrates a regulatory network that is conserved throughout animal evolution. We postulate that cytoplasmic polyadenylation through CPEBs was a fundamental innovation that contributed to animal evolution from unicellular life.

**Key words:** cytoplasmic polyadenylation, post-transcriptional regulation, evolution, Ctenophora, Cnidaria.

## Introduction

Post-transcriptional control of gene expression encompasses events that influence mRNA localization, stability, and rate of translation (Hentze 1995; Wickens et al. 1997; Mathews et al. 2007). Whereas gene expression can be regulated at many levels, post-transcriptional regulation of mRNA is known to be particularly relevant during early stages of animal development (Rosenthal et al. 1980; Wickens 1990; Curtis et al. 1995; de Moor et al. 2005; Lasko 2009; Richter and Lasko 2011), where the initial zygotic cleavages can occur from cytoplasmic material deposited in the egg and in the absence of nuclear components, including chromosomal DNA (Harvey 1936; Brachet et al. 1963). Instead of being driven by transcriptional events, changes in gene expression during ovulation and immediately after fertilization are orchestrated through cytoplasmic regulation of maternal transcripts. Post-transcriptional regulation of maternal mRNA results in timely production of proteins that control cell cycle progression and cell fate determination during early development (Hake and Richter 1997; Puoti et al. 1997; Crittenden et al. 2003; de Moor et al. 2005).

Cytoplasmic polyadenylation is a post-transcriptional mechanism for regulating gene expression that involves lengthening of the 3'-polyadenosine tail of mRNA (i.e., the poly(A)-tail) following nuclear polyadenylation and export from the nucleus (Wickens 1990; Wickens et al. 1997; Richter 1999; Mendez and Richter 2001; Weill et al. 2012; Charlesworth et al. 2013; Ivshina et al. 2014). Lengthening the poly(A)-tail through this mechanism correlates with stability and higher translational activity, whereas its shortening leads to dormancy and decay (Bachvarova 1992; Vassalli and Stutz 1995; Mangus et al. 2003). In contrast to canonical polyadenylation events that take place during transcriptional termination in the nucleus, which are part of the usual processing for the vast majority of eukaryotic mRNAs, cytoplasmic polyadenylation is limited to specific substrates and biological contexts (Ivshina et al. 2014; Yu and Kim 2020). This phenomenon was first documented, to our knowledge, during experimentally induced cleavage of enucleated sea urchin embryos (Wilt 1973). In the time since, studies of oogenesis and early embryonic development in a handful of bilaterian animal models have identified homologs of the

© The Author(s) 2023. Published by Oxford University Press on behalf of Society for Molecular Biology and Evolution.

This is an Open Access article distributed under the terms of the Creative Commons Attribution License (<https://creativecommons.org/licenses/by/4.0/>), which permits unrestricted reuse, distribution, and reproduction in any medium, provided the original work is properly cited.

Open Access

Cytoplasmic Polyadenylation Element-Binding Protein (CPEB) as conserved regulators for cytoplasmic polyadenylation of maternal mRNAs (Mendez and Richter 2001; Villalba et al. 2011; Ivshina et al. 2014). The best-characterized cytoplasmic polyadenylation complexes contain three primary components: a CPEB, a noncanonical poly(A) polymerase (e.g., GLD2), and subunits of the Cleavage and Polyadenylation Specificity Factor (CPSF) (fig. 1A). CPEBs provide substrate specificity to the complex (Hake et al. 1998; Afroz et al. 2014), whereas members of the GLD-2 family provide enzymatic activity (Wang et al. 2002; Barnard et al. 2004; Rouhana et al. 2005; Benoit et al. 2008). Cytoplasmic polyadenylation not only requires CPSF subunits but also a sequence element that these proteins recognize during transcriptional termination (the hexanucleotide AAUAAA; Bilger et al. 1994; Dickson et al. 1999), which because of its ubiquitous presence in mRNA that contributes negligibly to target selection in the cytoplasm.

CPEBs are divided into two major subfamilies. Members of the CPEB1 subfamily are required for oogenesis and regulation of maternal mRNAs during early development across Bilateria (Hake et al. 1998; Hasegawa et al. 2006; Racki and Richter 2006; Rouhana et al. 2017; Barr et al. 2019). For example, mutations in the *Drosophila* CPEB1 ortholog, *oo18 RNA binding (orb)*, obstructs oogenic progression during (null) and after (*orb*<sup>303</sup>) 16-cell cyst formation, whereas a less severe mutation (*orb*<sup>mel</sup>) results in abnormal embryonic development due to misregulation of localized mRNA translation (Christerson and McKearin 1994; Lantz et al. 1994; Chang et al. 2001). Members of the CPEB2 subfamily (e.g., CPEB2, CPEB3, and CPEB4 in mice and humans; Orb2 in *Drosophila*; and CPB-1 and FOG-1 in *Caenorhabditis elegans*) display enriched expression in animal testes, and some are known to be required for sperm development (Luitjens et al. 2000; Xu et al. 2012; Rouhana et al. 2017). Similarly, homologs of the catalytic subunit of the cytoplasmic polyadenylation complex (i.e., the GLD2 family of noncanonical poly(A) polymerases) are also required for oogenesis, spermatogenesis, and early embryonic development (Wang et al. 2002; Barnard et al. 2004; Benoit et al. 2008; Cui et al. 2008; Sartain et al. 2011; Norvell et al. 2015). Outside of the germline, CPEBs and GLD2 homologs have a conserved role in regulating localized translation of neuronal transcripts, and their function is required for memory formation and synaptic plasticity (Huang et al. 2002; Si, Giustetto et al. 2003; Keleman et al. 2007; Kwak et al. 2008; Majumdar et al. 2012; Udagawa et al. 2012; Chao et al. 2013; Pai et al. 2013).

The C-terminus of CPEBs contains a highly conserved RNA-Binding Domain (RBD), which is composed of two RNA recognition motifs (RRMs) and a Zinc Finger (fig. 1B). The RBD of CPEBs from bilaterian phyla (Deuterostomia, Lophotrochozoa, and Ecdysozoa) contains primary structure that is more than 30% identical (Rouhana et al. 2017), whereas the rest of the protein lacks recognizable sequence conservation (fig. 1B; reviewed by Kozlov et al. (2021)). CPEB1 orthologs bind to well-defined Cytoplasmic Polyadenylation Elements (CPEs; consensus sequence: UUUUA(U/A)) present in the 3' UTR of their targets, which include *c-mos*, *cyclin*, and *Dazl*

mRNAs (Fox et al. 1989; McGrew and Richter 1990; Stebbins-Boaz et al. 1996; de Moor and Richter 1999; Tay et al. 2000; Pique et al. 2008; Chen et al. 2011). There is less conservation or agreement regarding sequence recognition by members of the CPEB2 subfamily in comparison to that of CPEB1, but these also seem to have affinity for U-rich elements (Huang et al. 2006; Stepien et al. 2016; Duran-Arque et al. 2022). Evidence exists for co-regulation of some targets of cytoplasmic polyadenylation by members of both CPEB subfamilies (Pique et al. 2008; Hagele et al. 2009; Giangarra et al. 2015; Calderone et al. 2016), as well as for functions of CPEBs that are independent of poly(A)-tail modulation (Minshall et al. 2007; Lin et al. 2010; Chen and Huang 2012; Kruttner et al. 2012). However, the majority of studies show that the central role of CPEBs is in regulating specific subsets of mRNA via cytoplasmic regulation of poly(A) tail length (Radford et al. 2008; Kronja and Orr-Weaver 2011; Villalba et al. 2011; Darnell and Richter 2012; Fernandez-Miranda and Mendez 2012; Charlesworth et al. 2013; Ivshina et al. 2014).

Despite its important regulatory role in animal development, it is not known whether cytoplasmic polyadenylation is present in non-bilaterian animals. Homologs of GLD2 and CPSF subunits are present across Eukarya and involved in nuclear processes (Kwak et al. 2004; Dominski and Marzluff 2007; Preston et al. 2019). However, a recent global survey determined that CPEB homologs are absent outside of animals and present in genomes from every major animal lineage (see supplementary table S1, Supplementary Material online) (Paps and Holland 2018). These findings are consistent with the hypothesis that cytoplasmic polyadenylation arose in the lineage leading to the last common ancestor of animals. However, the results relied on similarity-based methods and require phylogenetic confirmation as well as functional evidence. Here we phylogenetically analyze the presence of CPEB1 and CPEB2 subfamily members in genomes of species that belong to each of the five major animal lineages, which are bilaterians (that account for 99% of all extant animal species) and the four earlier branching non-bilaterian clades (ctenophores, placozoans, sponges, and cnidarians), as well as in genomes of non-metazoan models. We also assess whether CPEBs and other members of the cytoplasmic polyadenylation complex are maternally deposited in eggs of the cnidarian model *Nematostella vectensis* and the ctenophore *Mnemiopsis leidyi*. Finally, we determine whether CPEB targets identified in studies of maternal mRNA regulation in vertebrate models display conserved changes in poly(A)-tail length during oocyte maturation and early embryonic development in cnidarians and ctenophores. Our findings suggest that CPEB-mediated cytoplasmic polyadenylation is an ancestral mechanism that regulates timely expression of a genetic network that contributes to early development across animals.

## Results

### CPEB Phylogeny

We used the RBD domain of human CPEB1 (NP\_001275748.1; AA 234–479) as input in TblastN

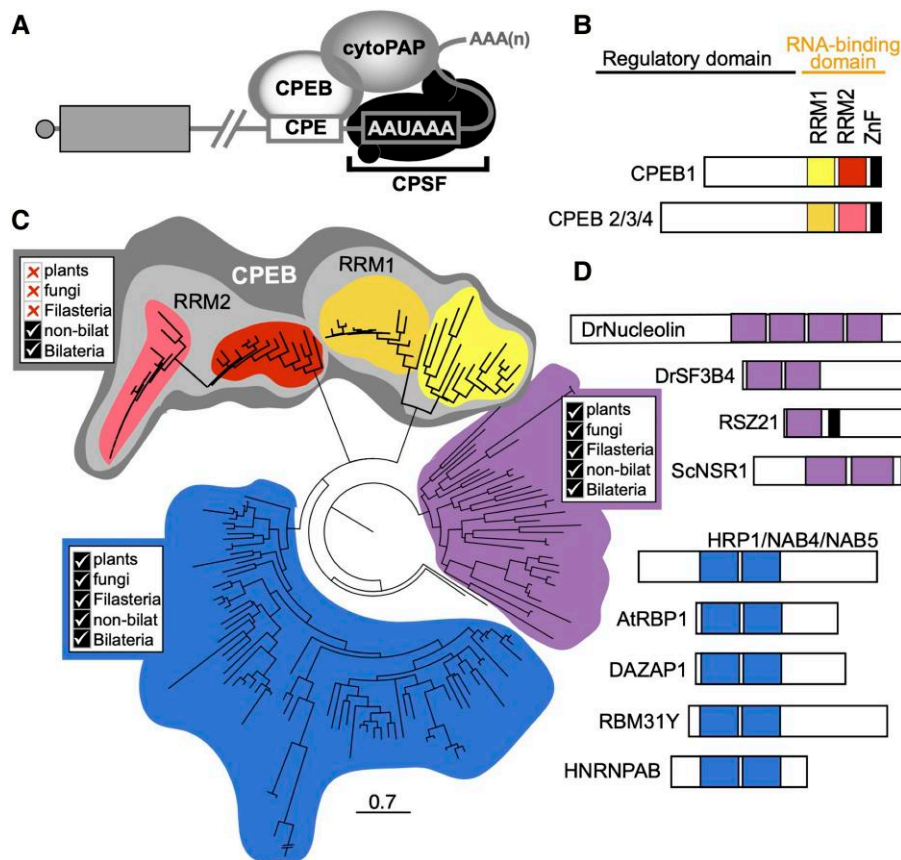


**Fig. 1.** Cytoplasmic Polyadenylation Element-Binding Proteins (CPEBs) are highly conserved post-transcriptional regulators present at the stem of animal evolution. (A) Diagram depicting the core cytoplasmic polyadenylation complex. Subunits of the CPSF are bound to the hexanucleotide  $A_2UA_3$ , and a CPEB bound to Cytoplasmic Polyadenylation Elements (CPEs) recruits a poly(A) polymerase of the GLD2 family (cytoPAP) to the 3'-end of mRNAs. (B) CPEBs contain a highly conserved C-terminal RNA-binding domain composed of two RNA recognition motifs (RRMs; yellow for RRM1 and red for RRM2 of CPEB1; orange for RRM1 and pink for RRM2 of CPEB2/3/4 subfamily members) and a Zinc-Finger motif (ZnF; black). The N-terminus of CPEBs is not well conserved but is known to contain regulatory elements. Diagram based on representatives from *Schmidtea mediterranea* (Rouhana et al. 2017). (C) Maximum-likelihood phylogenetic tree based on similarity to individual RRM1 and second (RRM2) RNA recognition motifs of previously characterized CPEBs (e.g., *Mus musculus* CPEB1-4) positioned in separate clades (light gray shading) that were only composed of metazoan sequences (color coding for subclades correspond to those used for respective RRM1 and RRM2 motifs in panel (B)). Proteins from nonanimal species, such as plant, fungi, and choanoflagellates, are only found in clades that lacked CPEBs (shaded in blue and purple). (D) Bar diagrams of representative proteins in clades with homology to RRM1 and RRM2 motifs of CPEBs. RRM1 and RRM2 motifs are depicted in the color shading of their corresponding clades in panel (C) and ZnF shown in black. Scale bar represents substitutions per amino acid position.

searches ( $e$ -value cutoff = 0.05) against gene models of the following animal species: *Amphimedon queenslandica* (Porifera), *M. leidy* (Ctenophora), *N. vectensis* (Cnidaria), *Trichoplax adhaerens* (Placozoa), *Drosophila melanogaster* (Arthropoda), *Capitella teleta* (Annelida), *Schmidtea mediterranea* (Platyhelminthes), as well as *Mus musculus* and *Danio rerio* (Chordata). We also used the same query to search gene models from the following nonanimal relatives: *Saccharomyces cerevisiae* and *Schizosaccharomyces pombe* (Fungi), *Arabidopsis thaliana* (Plantae), *Capsaspora owczarzaki* (Filasterea), and *Salpingoeca rosetta* (Choanoflagellata). We detected sequences with RBD domains from all species except *C. owczarzaki* under the used parameters. After condensing genes with multiple isoforms down to one representative, we constructed an alignment of individual RRM1 and RRM2 motifs (supplementary file S1, Supplementary Material online) and used it to infer the

phylogenetic relationships amongst individual RRM1 and RRM2 motifs present in CPEBs and related non-CPEB sequences. The RRM1 and RRM2 motifs of previously characterized CPEBs from *Drosophila*, the planarian *S. mediterranea*, and vertebrate species clustered together with hits that were exclusively from animal lineages (figs. 1C and S1, Supplementary Material online). Sequences from nonanimal lineages, including plant, fungi, and the choanoflagellate *S. rosetta*, were absent from clades that included RRM1 and RRM2 motifs from CPEB orthologs (figs. 1C and S1, Supplementary Material online). Our results indicate that CPEBs are found in every major animal lineage and are specific to animals.

In addition to finding CPEBs in every major animal lineage, at least one ortholog each of CPEB1 and CPEB2 were identified in every metazoan species that we surveyed including Ctenophora and Porifera. This indicates that both CPEB1 and CPEB2 subfamilies were present in the

genome of the last common ancestor of extant metazoans and suggests that the presence of both CPEB1 and CPEB2 is critical for most if not all animals. Notably, sequences corresponding to the first RRM (RRM1) of both CPEB1 and CPEB2 proteins clustered separately from those corresponding to the second RRM (RRM2) in all CPEBs (fig. 1C), indicating that CPEB1 and CPEB2 subfamilies share a common origin and conserve an ancestral architecture with tandem RRMs. Our parallel analysis using the Zinc-Finger domain present in CPEBs (supplementary fig. S2, Supplementary Material online) was congruent with our analyses of the RRM domains.

The closest neighboring clade of RRMs to those of CPEBs contains factors known to be involved in post-transcriptional regulation of maternal mRNAs in bilaterians, including Squid and Musashi, DAZ-Associated Protein-1 (DAZAP-1), and Heterogeneous nuclear ribonucleoprotein 27C (Hrb27C) orthologs. Musashi cooperates with CPEB in regulating cytoplasmic polyadenylation activity during vertebrate oocyte maturation (Charlesworth et al. 2006; Rutledge et al. 2014; Weill et al. 2017), whereas DAZAP-1 binds to DAZL (Dai et al. 2001), which also cooperates with CPEB during oocyte maturation (Sousa Martins et al. 2016). This clade also includes proteins from yeast, plant, and nonanimal species closely related to metazoans, such as HRP1/YOL123W (which is required for 3'-end formation in *S. cerevisiae*; Kessler et al. 1997), and heterogeneous nuclear ribonucleoproteins (hnRNPs) that participate in pre-mRNA splicing, mRNA transport, and RNA editing (Dreyfuss 1986; Geuens et al. 2016). These proteins share a similar architecture as CPEBs in that they contain two RRMs in tandem, although these are positioned near the N-terminus rather than the C-terminus and lack a Zinc Finger (fig. 1D). As with CPEBs, members of this clade have RRMs that cluster into separate subclades (RRM1 and RRM2; fig. 1C). However, unlike CPEBs, these subclades were composed of sequences from different kingdoms, which suggests that these proteins were present in the last common eukaryotic ancestor. The third and last major clade found in our analysis included RRMs from orthologs of Nucleolin, which is a major regulator of rRNA biogenesis conserved in plants, yeast, and animals (reviewed by Tajrishi et al. (2011), as well as splicing factors RSZ21 and RSZ22 from *A. thaliana* (fig. 1C). Altogether, these results support the hypothesis that CPEBs are a family of proteins exclusively present in animals. Additionally, these results suggest that CPEBs share ancestry with Musashi and DAZAP, and ultimately arose from heteronuclear RNA-binding proteins ubiquitously present in eukaryotes.

### Analysis of Maternal mRNA Regulation by Cytoplasmic Polyadenylation in Cnidaria

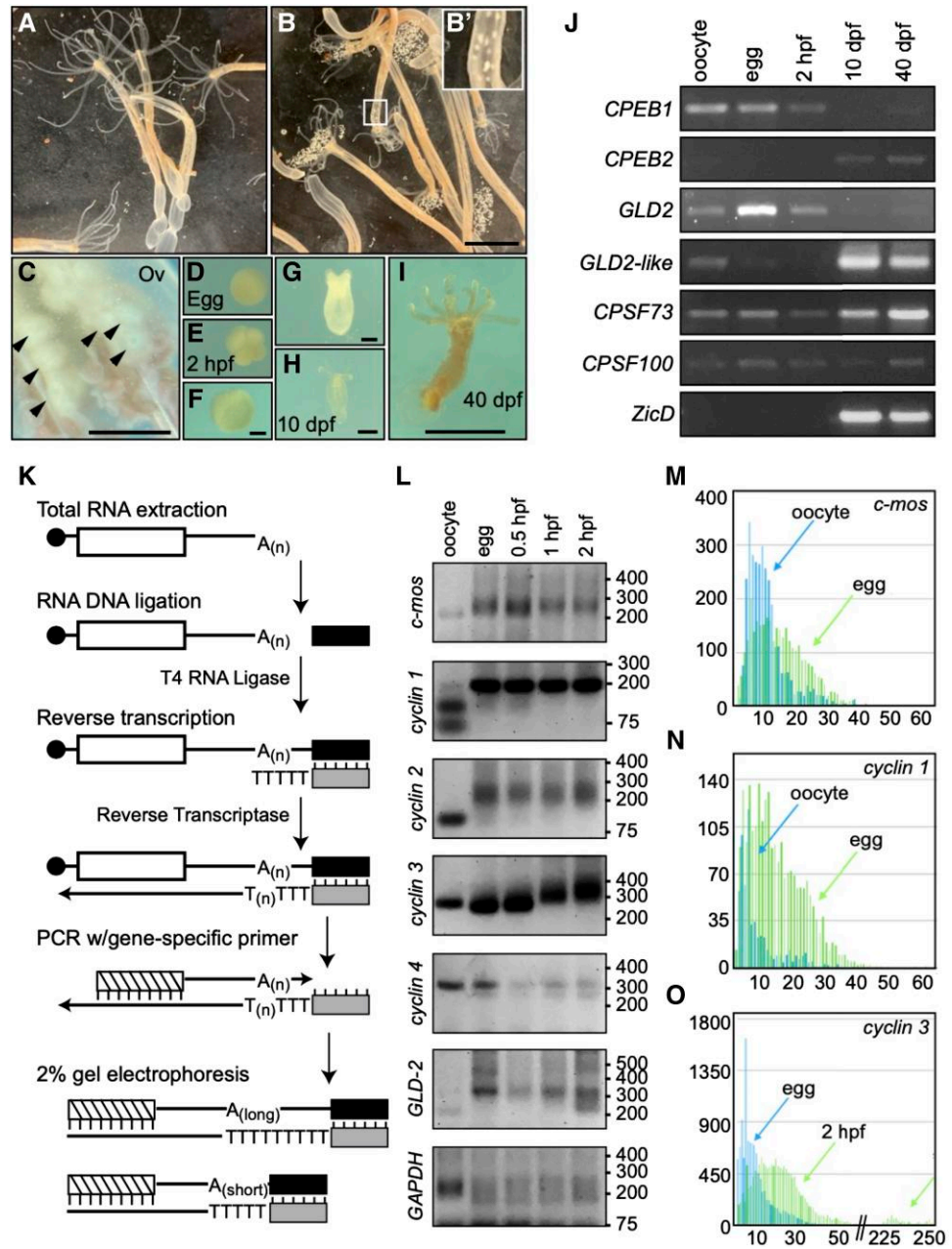
To test for evidence of cytoplasmic polyadenylation in cnidarian species, we extracted RNA from the ovaries, spawned eggs, embryos, and adult polyps of the sea anemone *N. vectensis* at different timepoints postfertilization, and determined the expression of core cytoplasmic polyadenylation machinery components using reverse transcription PCR

(RT-PCR; fig. 2A–J). Expression of CPEB1 and GLD2 orthologs was readily detectable in the oocyte, the egg, and immediately postfertilization, but declined at later stages of development (fig. 2J). Expression of the CPEB2 ortholog and a second GLD2 homolog (*NvGLD2-like*) were most obvious in samples obtained 10- and 40-days postfertilization (dpf), which correlated the timing of expression of the neuronal and neuronal ectoderm marker *NvZicD* (fig. 2J; Layden et al. 2010). Expression of CPSF subunits (*NvCPSF73* and *NvCPSF100*) was detected at every tested timepoint, as would be expected of factors that are involved with canonical 3'-end processing and polyadenylation in the nucleus (fig. 2J). In the absence of available antibodies to determine the presence of factors at the protein level, these results show expression of the cytoplasmic polyadenylation machinery in late oogenesis and early embryogenesis of *N. vectensis*, indicating that this is indeed a conserved feature between cnidarians and bilaterians.

To determine whether long poly(A) tails result in increased translation products in *N. vectensis* eggs and embryos, we utilized a dual NanoLuc/Firefly luciferase reporter system (Sheets 2019). We used in vitro transcription to generate NanoLuc mRNAs with and without poly(A) tails of ~100 to ~350 adenosines in length, which is close to the initial length of ~250 nucleotides observed in mammalian cells (Kuhn et al. 2009), and injected these into *N. vectensis* eggs and embryos (supplementary fig. S3, Supplementary Material online). We generated luciferase mRNAs lacking a poly(A) tail in the same manner and co-injected these as loading controls. Upon 6 h postinjection, levels of NanoLuc and luciferase activity indicated that polyadenylated mRNAs generated up to 30-fold more product than those lacking a poly(A) tail in both eggs and embryos (supplementary fig. S3, Supplementary Material online). To determine whether increased NanoLuc signal from polyadenylated reporters was due to higher mRNA stability, higher translational efficiency, or both, we compared the abundance of NanoLuc mRNA by reverse transcription quantitative PCR (RT-qPCR) in *Nematostella* eggs injected 6 h prior. We observed that the absence of a poly(A)-tail did not result in decreased stability of reporter mRNAs under these conditions (supplementary fig. S3D, Supplementary Material online). However, NanoLuc activity measured 6 h postinjection in the same batch of injected eggs was over 10-fold higher for polyadenylated mRNAs than for counterparts lacking a poly(A) tail (supplementary fig. S3E and F, Supplementary Material online). These data show that the presence of a poly(A) tail stimulates translation in *N. vectensis* eggs and embryos, as is known to occur during early development of bilaterians (Vassalli et al. 1989; Salles et al. 1994; Sheets et al. 1994; Barkoff et al. 1998).

Next, we looked for evidence of poly(A) tail lengthening during ovulation and early embryonic development of *N. vectensis*. To do this, we identified *N. vectensis* homologs of known CPEB substrates, and measured poly(A) tail length of their mRNA using a well-established PCR-based assay (fig. 2K; Charlesworth et al. 2004; Rouhana and Wickens 2007). Briefly, total RNA was extracted from dissected

**Fig. 2.** Cytoplasmic polyadenylation during oocyte maturation and early development of *Nematostella vectensis*. (A–I) Bright field images of *N. vectensis* reproductive process. Females before (A) and after spawning (B). Inset shows migration of eggs through column during ovulation (B'). Magnified view of ovaries (Ov; C), an egg (D), early cleavage (E), gastrula (F), tentacle bud stage (G), juvenile polyp (unfed; H), and polyp after multiple feedings (I). hpf, approximate hours postfertilization at room temperature; dpf, days postfertilization. Scale bars = 1 cm, B; 1 mm, C and I; 0.1 mm, F–H. (J) Developmentally regulated expression of cytoplasmic polyadenylation components detected by RT-PCR. (K) PCR-based assay for measurement of poly(A) tail length. Total RNA extracted from specific tissues and developmental stages was ligated to the 5'-end of a DNA oligo and used as a template for reverse transcription using a primer annealed to the ligated DNA oligo. The synthesized cDNA containing the poly(A) region was then used as template to amplify the 3'-end of mRNAs of interest using a gene-specific primer and the primer antisense to the ligated DNA oligo. Changes in poly(A) tail length were assessed by differences in electrophoretic mobility of PCR products in a 2% agarose gel. See Materials and Methods section for more details. (L) Assessment of shifts in electrophoretic mobility representative of changes in poly(A) length for gene-specific transcripts using the assay shown in (K). Size of DNA markers is shown on the right. (M–O) Bar graphs depicting number of Amplicon-EZ reads (x-axis) for each specific length of poly(A) tail (y-axis) in *c-mos* (M), *cyclin1* (N), and *cyclin3* (O) mRNAs. Reads from oocytes are shown in blue and eggs in green in (M and N), whereas reads from eggs are shown in blue and those from embryos 2-hpf are shown in green in (O).



oocytes, eggs, and embryos at 0.5, 1, and 2-h postfertilization (hpf), and ligated with a DNA oligo at the 3'-end of the RNA. Then, a complementary oligo with a dT<sub>(5)</sub> extension at its 3'-end was used in a reverse transcription reaction selective for polyadenylated transcripts. The resulting cDNA was used as template for PCR using a gene-specific forward primer and a reverse primer identical to the one used for reverse transcription. Because the reverse primer anneals to the oligo originally ligated at the end of the transcripts, the presence of longer poly(A) tails results in upward shifts in electrophoretic motility when compared with shorter poly(A) tails on otherwise identical mRNAs (fig. 2K). Using this approach, we detected mRNA tail elongation for five conserved CPEB substrates (fig. 2L). Homologs of cell cycle regulators *c-mos* (*Nv\_c-mos*) and *cyclin A* and *B* homologs (*Nv\_cyclin1* and *Nv\_cyclin2*, respectively) displayed longer poly(A) tails in the egg than in the oocyte (fig. 2L), matching what is known to occur during oocyte meiotic maturation in *Xenopus* (Sheets et al. 1994). The maternally expressed cytoplasmic poly(A) polymerase ortholog *NvGLD2*, likewise displayed an increase in poly(A) tail length during meiotic maturation (fig. 2L), which is also observed in *Xenopus* (Rouhana and Wickens 2007). A third cyclin homolog, *Nv\_cyclin3* (closest human homolog being cyclin B3), was polyadenylated upon fertilization, most noticeably between 0.5- and 1-hpf (fig. 2L). Conversely, the poly(A) tail of mRNAs encoding for a fourth cyclin homolog (*Nv\_cyclin4*), as well as the housekeeping gene *GAPDH*, either stayed constant or shortened as development progressed (fig. 2L). We verified that the electrophoretic motility of amplicons from polyadenylated transcripts matched the size predicted based on the position of the gene-specific primer, the length of 3'-ends (according to 3'UTR reads deposited at the Stowers Institute for Medical Research repository [simrbase.stowers.org] and the National Center for Biotechnology Information [NCBI; [www.ncbi.nlm.nih.gov](http://www.ncbi.nlm.nih.gov)], plus potential poly(A) tails), and the ligated 3'-end adapter (table 1 and supplementary fig. S4, Supplementary Material online). This process also revealed the presence of canonical CPEs in the 3'UTR of each of the polyadenylated mRNAs (supplementary fig. S4, Supplementary Material online). Altogether, these results show dynamic lengthening and shortening of maternal mRNAs of *Nematostella* in a manner that parallels behaviors observed during early development of bilaterians. The increases of poly(A) tail length observed in *N. vectensis* *c-mos*, *GLD-2*, and *cyclin1*, 2, and 3 homologs, as well as the presence of CPEs in their 3'UTRs, support the hypothesis that CPEB-mediated polyadenylation during meiotic maturation and early development is part of a conserved genetic program that predates the last common ancestor of cnidarians and bilaterians.

We sought to validate the identity of amplicons produced in our poly(A) tail length assay directly by Sanger sequencing fragments cloned into bacterial vectors. During this process, we verified the identity of our PCR products and presence of poly(A) tails of different lengths (supplementary figs. S4 and S5, Supplementary Material online). We also observed evidence of non-templated

incorporation of uridine and guanosines within the poly(A) of some transcripts (supplementary fig. S5, Supplementary Material online). To investigate the changes in length and composition of poly(A) tails represented in our PCR-based assay in more depth, we analyzed hundreds of amplicon sequences for *c-mos*, *cyclin1*, and *cyclin3* mRNAs using Illumina Next-Generation sequencing of PCR amplicons (Amplicon-EZ, Genewiz, Azenta Life Sciences, South Plainfield, NJ; supplementary fig. S6, Supplementary Material online). Cognizant of the caveats that sequencing through long stretches of polynucleotide repeats is difficult, and that measurements using sequencing approaches tend to underestimate the precise length of poly(A) tails (Quail et al. 2012; Zheng and Tian 2014), we designed a program that selects for tail sequence represented in both forward and reverse Amplicon-EZ reads (get\_polya.pl, in GitHub repository). This program trims generic sequence and potential sequencing errors and calculates the number of non-templated positions at the 3'-end of mRNAs represented in our Amplicon-EZ reads (supplementary File S2, Supplementary Material online). Using this approach, we detected extension of poly(A) tail length during oocyte maturation for *c-mos* and *cyclin1*, as well as after fertilization for *cyclin3*. For *c-mos*, we detected an increase in poly(A) tail length from a mean of 10 nucleotides in oocytes to 15 nucleotides using this method (median 9 and 13 nucleotides, respectively; figs. 2M and S6, Supplementary Material online). Likewise, we detected an increase in mean from 8 to 14 nucleotides for *cyclin1* (median of 5–12 nucleotides, respectively; figs. 2N and S6, Supplementary Material online) and from 9 nucleotides in the egg to 38 nucleotides in embryos 2-hpf for *cyclin3* (median 7 and 20 nucleotides; figs. 2O and S6, Supplementary Material online). Interestingly, two peaks of poly(A) tail length (at median 19 and 247 nucleotides) were observed when plotting the length of *cyclin3* poly(A) tail at the latter developmental timepoint (2-hpf; fig. 2O), suggesting a potential heterogenous population of cytoplasmic polyadenylation products from the same gene. Overall, we observed a trend of poly(A) tail lengthening in developmental timepoints that correlates with those observed by gel electrophoresis for all three genes (fig. 2L), indicating that the shifts in electrophoretic motility of amplicons observed in our original PCR-based poly(A) tail assays are due to changes in poly(A) tail length.

The analysis of nucleotide composition of poly(A) tails from Amplicon-EZ data revealed that adenines were by far the most prevalent base, encompassing ~76% of all positions in the tail (supplementary table S2, Supplementary Material online). Uridine was the second highest by occupying ~16% of all positions. Guanines and cytosines composed ~5% and ~3%, respectively. We observed differences in composition between the 5' and 3' regions of the tail, with uridine enrichment at immediate positions after the cleavage and polyadenylation site (supplementary table S2, Supplementary Material online). To visualize the mixed composition of the 5'-end of these tails, we depicted the frequency of each nucleotide in the first 20 positions of untemplated sequence for

**Table 1.** Oligonucleotides Used in This Study.

Identifier (GenBank ID)	Gene	Forward primer	Reverse primer	Ta
<i>N. vectensis</i>				
Nv_CPEB1	Nv_CPEB1	ATGGCCGGATCTATGCCGACACCCCTGG	TCACATGGTGAGCTGGTCTCGACTTGC	58 °C
Nv_CPEB2	Nv_CPEB2	ATGGCCGATTTGGCCAGAAACAAGATC	TCACCACCTGAAGGGCACCCGTGGTCTGTCTGC	58 °C
(XM_032362260.1)	Nv_GLD2	AGAGCCGCATTTCTCGAAGATTACACCC	CCTGATTTGTGCAGTATTTACAGATAGCTCTTCCAG	58 °C
NvERTx.4.14958	Nv_GLD2-like	ATGCAGAGAACCCTACACTAGCTTAGCCAGG	CTACATGATGTCATTTAACTCCGCCCTATGCG	58 °C
(XM_032380547.1)	Nv_CPSF73	ATGGCCGCTCCGTAAGCCGAAAGGCTGAC	TCAGCTGAAGATGGCCGTGAAGGGCGGAG	58 °C
(XM_032363231.1)	Nv_CPSF100	ACGTCATTATTAAGCTAAATGTCTCTCGGAGCC CACGGAAGACACCTCTGTG	CTAGACAATAGCATTTGTGAATACAGAAGGTCCCG	58 °C
(XM_032375916.1)	Nv_ZicD	ATGACCCGGCACAGCAAAACGGACAGCATTGGC	TTAGCACAGTAGTACCACCTTGTGGCTTTGCTTTTAGC	58 °C
(XM_001629488.2)	Nv_c-mos PAT	CATTTGGCCGTCATAGTCATCC		55 °C
NvERTx.4.87874	Nv_cyclin1 PAT	CCATGTAGATTCCATATCCCAAGAGG		56 °C
NvERTx.4.58222	Nv_cyclin2 PAT	GCTACATGGACCTTGTGTCCAG		56 °C
NvERTx.4.144958	Nv_cyclin3 PAT	GTGGCATTAGTACTCATTCAAGGG		56 °C
NvERTx.4.149292	Nv_cyclin4 PAT	GCTATGCATGATGAAAGAAAGCTTG		56 °C
(XM_032362260.1)	Nv_GLD-2 PAT	CAGCGTCTACTCCAGACAG		55 °C
NvERTx.4.200370	Nv_GAPDH PAT	AACTGTAGTAGGAGATACTAGCC		55 °C
<i>M. leidyi</i>				
ML042716a	MI_CPEB1a	GTACCCGGTTCTACGTTTGTCC	TCCTCTCTCGTCCGATGTCAGG	56 °C
ML05853a	MI_CPEB1b	TAGCATGTTCCGAAAGTTTGGTGG	TGGGGACATACACTTGACTTGAC	56 °C
ML05854a	MI_CPEB1c	TGCAACATCATGTGACCAAAAGTGG	TGAATTTCCGTAGGATCAGCGAAC	56 °C
ML05855a	MI_CPEB1d	CTTAAAAGTTGCGAGTTGTTGTCC	CATATGCAGCAACTGACCCATCG	56 °C
ML05856a	MI_CPEB1e	TGCAATCAGAACACTACCAC	TTTGACATGCTTGTACCGATTGC	56 °C
ML033245a	MI_CPEB1f	CGAACGATTAATCAGGGGAGACAAC	TTGGTAATTGTTGGCACCTGTCC	56 °C
ML03369a	MI_CPEB2	CAGCAGTTTGGAAATTCGTCTGGTC	GGAACCGGTACCTTTTGTATGGAATG	56 °C
ML08889a	MI_GLD2	AGCTGCAGATTAAAGTCCCGAAC	CTGATAAACCCGGGCTATTCTGACG	56 °C
ML005010a	MI_GLD2b	TGTTAAAGCGTGGGCAAAAGTCC	TTTCATCATGTTGCACGTCCTCG	56 °C
(JF912806.1)	MI_islet	AGGTTTCTGTCCAACGATTTCCG	CATGCTCTGATTTGAGTCTGCTCCTC	56 °C
ML015751a	MI_cyclin homolog (2) PAT	TAGAGTGTGGTGAGACCTGG		55 °C
ML455312a	MI_cyclin homolog (4) PAT	CCTACCTTATTAGTAGAATAGTGTCCG		55 °C
ML46822a	MI_cyclin homolog (5) PAT	ACGGTTGAATCTAGACATTTGG		55 °C
ML049317a	MI_cyclin homolog (6) PAT	CCAGTGTGTAATCGAGCTATG		55 °C
ML05854a	MI_CPEB1c (ISH probe)	TGCCAATGCTCTTTCTCCAA	CGACAATTGCATGAGATGCT	48 °C
GB135	-	Phos-GGTCACTGATCTGAAGC-Amine		
GB136_T5	-	GCTTCAGATCAAGGTGACCTTTTT		
Amplicon-EZ				
AmpNvMos	Nv_c-mos (for PAT	acactcttccctca cga cgc tct ccc gat cct CATTTGCGCGCTCATAGTCATCG		56 °C
	Amplicon-EZ)			
AmpNvCyclin1	Nv_cyclin1 (for PAT	acactcttccctca cga cgc tct ccc gat cct CCATGTAGATCCCATATCCCAAGAGG		56 °C
	Amplicon-EZ)			
AmpNvCyclin3	Nv_cyclin3 (for PAT	acactcttccctca cga cgc tct ccc gat cct GTGGCATTAGTACTCATTCAAGGG		56 °C
	Amplicon-EZ)			
AmpliconSeqGB136T5	GB136T5 (for PAT	gactggagtrcagagtgctctccgatctGCTTCAGATCAAGGTGACCTTTTT		56 °C
	Amplicon-EZ)			
Reporter RT-qPCR	Firefly luciferase	CAACACCCCAACATCTTCCGACG	TGGCCACATAGTCCACGATCTC	55 °C
	Nanoluc luciferase	ATCCCGTATGAAGGTCTGAGCG	AACCCCGTCCGATTACCAGTGTG	55 °C

The sequence of oligonucleotides used as primers for gene-specific amplification of cDNA (VND) of c-mos (forward and reverse), as well as poly(A) tail length assays (PAT) and reverse transcription quantitative PCR (RT-qPCR), are listed along with corresponding annealing temperatures (Ta).

tails of at least 5 nucleotides (nts) using the WebLogo sequence generator (Crooks et al. 2004). Using this approach, we observed similar occupancy of uridines and adenines at the first position of the tail, with gradual decreases in prevalence of uridine moving downstream (supplementary fig. S6, Supplementary Material online). Because the high presence of uridine at initial positions of the tail was not as prevalent in sequenced cDNA clones (supplementary fig. S5, Supplementary Material online), we performed additional tail composition analysis using *N. vectensis* egg RNA using Illumina RNAseq reads from ribodepleted samples (supplementary fig. S7, Supplementary Material online), as well as Nanopore direct RNA sequencing (supplementary fig. S8, Supplementary Material online). We found that reads representing *c-mos*, *cyclin1*, and *cyclin2* mRNAs in Illumina sequences included uridines within their poly(A) tails (supplementary fig. S7, Supplementary Material online). However, the presence of uridine in the first or second position of the tail in Illumina reads was only observed once each in >30 reads. Furthermore, uridines were absent in all the poly(A) tails corresponding to *cyclin3* mRNA (supplementary fig. S7, Supplementary Material online), suggesting that incorporation of oligouridine may not be as prevalent as represented in Amplicon-EZ reads. Sequences obtained using Nanopore technology had adenosines as the most prevalent base, but uridines were also present in most tails of analyzed mRNAs (12/13 for *c-mos*; 21/32 for *cyclin1*, and 30/38 for *cyclin3*; supplementary fig. S8, Supplementary Material online). Uridines were found throughout the tail and not enriched at either end in sequences obtained using this technology (supplementary fig. S8, Supplementary Material online). Whereas lack of correlation regarding the distribution of non-adenosine bases within the tail of mRNAs prohibits conclusive interpretation of these data, the frequent observation of mixed tails using four different approaches merits future investigation. Nevertheless, our data using RNA extracted from different developmental stages analyzed in parallel by electrophoretic mobility, as well as Sanger and Amplicon-EZ sequencing, clearly indicate that poly(A) tail lengthening for *cyclin* and *c-mos* mRNAs takes place during oogenesis and early development in *N. vectensis*.

### Analysis of Cytoplasmic Polyadenylation in Ctenophores

Our phylogenetic analyses revealed the existence of CPEB1 and CPEB2 orthologs in the genome of the ctenophore *M. leidy* (figs. 1C, S1, and S2, Supplementary Material online). We identified six *M. leidy* genes grouped as members of CPEB1 subfamily (figs. 1C, S1, and S2, Supplementary Material online), which was surprising because the CPEB1 family is most often represented by a single gene in previously analyzed species. To determine where within Ctenophora the CPEB1 expansion occurred, we looked for CPEB homologs in the genomes of *Hormiphora californensis* (Schultz et al. 2021) and *Beroe ovata* (Hernandez, Ryan, et al., unpublished). In both of these ctenophore genomes, we identified

one CPEB2 and six CPEB1 sequences (supplementary table S3 and supplementary fig. S9, Supplementary Material online). These results suggest that the expansion of CPEB1 occurred in the last common ancestor of these three ctenophores and has been maintained in all three lineages.

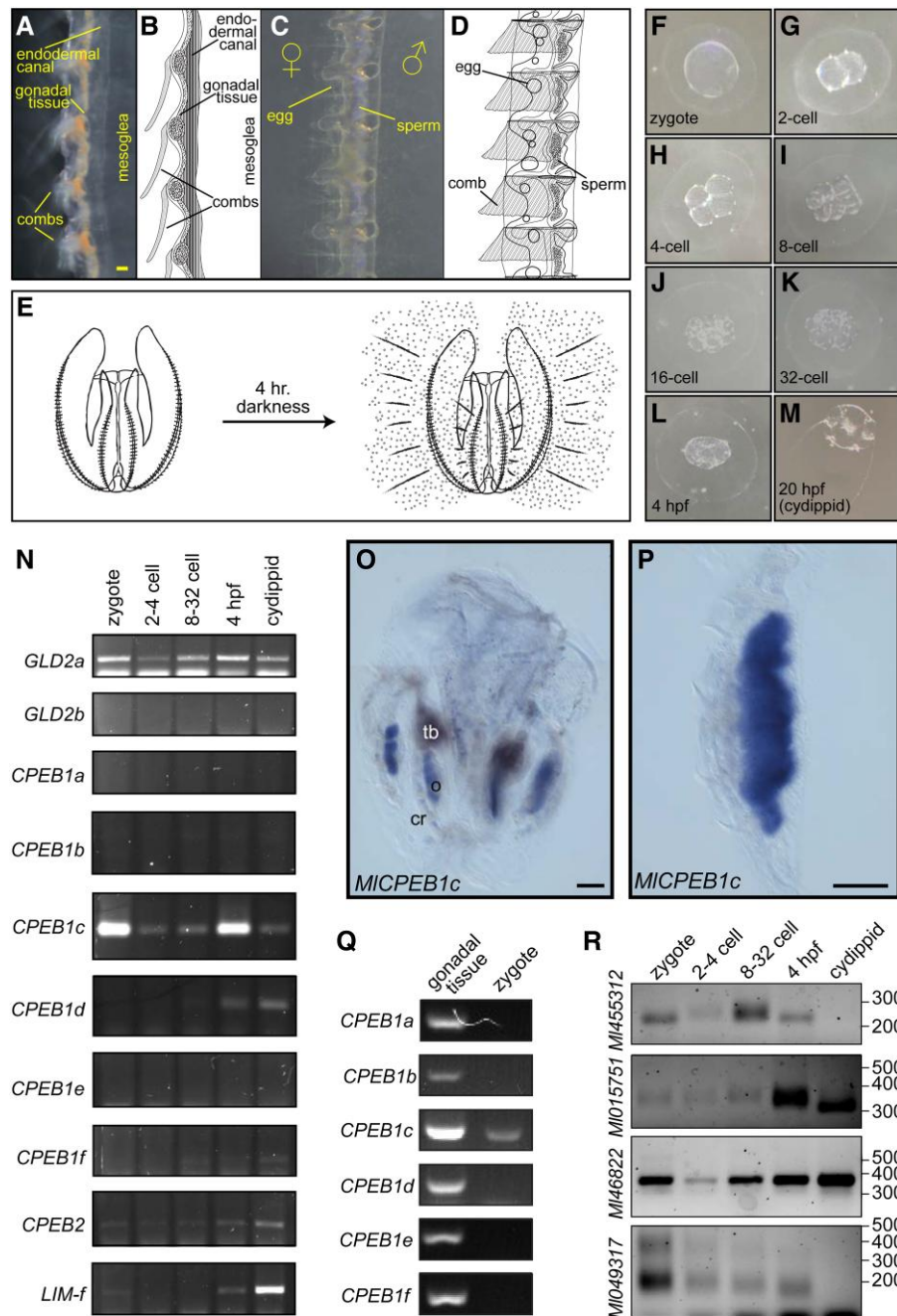
We next asked whether maternal expression of the CPEB1 ortholog and components of the cytoplasmic polyadenylation complex is a conserved feature in *M. leidy*. Most ctenophores, including *M. leidy*, are hermaphrodites that develop both testes and ovaries parallel to each other under each of eight comb rows that are aligned along the oral–aboral axis (fig. 3A–D). The presence of mesoglea and proximity of comb plates make it difficult to specifically isolate oocytes or ovarian tissue (fig. 3A and B). In addition, *M. leidy* is able to self-fertilize very effectively (Fischer et al. 2014) prohibiting analysis of unfertilized eggs. However, hundreds of synchronized embryos can be obtained following controlled spawning events in the laboratory (fig. 3E; Pang and Martindale 2008; Sasson and Ryan 2016). Upon spawning, cleavage occurs every 15–20 min (fig. 3F–K), and gastrulation can be observed by 4-hpf (fig. 3L). The juvenile cydippid stage is achieved by 20-hpf (fig. 3M), at which point specimens can eat, grow, and eventually develop gametes.

We extracted RNA from embryos collected as zygotes, combined 2- to 4-cell stages, combined 8- to 32-cell stages, and 4-hpf, to assess expression of CPEBs by RT-PCR. We also included RNA extracted from unfed cydippids in our analyses as control for the absence of maternal products and expression of markers for differentiated tissue. Using gene-specific primers, we detected maternal expression of one CPEB1 paralog (*MICPEB1c*; identifier ML05854a in the *Mnemiopsis* Genome Project Portal (Moreland et al. 2020)) and one of two GLD2 cytoplasmic poly(A) polymerase homologs (*MIGLD2a*; ML0889a) in zygotes (fig. 3N). Expression of four of the six CPEB1 paralogs (*MICPEB1a*/ML042716; *MICPEB1b*/ML05853a; *MICPEB1e*/ML05856a; and *MICPEB1f*/ML033245a) was not conclusively detected at any stage, nor was expression of a second GLD2 homolog (*MIGLD2b*/ML005010a). *MICPEB1d* (ML05855a) and the CPEB2 ortholog (*MICPEB2*/ML03369a) were both detected at the 4-hpf timepoint and in cydippids, but not during earlier stages of development (fig. 3N). The timing of expression of *MICPEB1d* and *MIGLD2b* mimics the expression of *ML\_islet* (ML053012a), a LIM family gene expressed in ectoderm and the apical organ of cydippids (Simmons et al. 2012). These results indicate that at least one member of the CPEB1 family and one GLD2 poly(A) polymerase are maternally expressed in *M. leidy*.

We sought to determine whether *MICPEB1c* is expressed maternally by direct analysis on developing oocytes. To do so, we obtained sexually mature *M. leidy* cydippids that had visible gonads and determined the distribution of expression of *MICPEB1c* by whole-mount in situ hybridization (fig. 3O and P). Using this approach, we observed robust expression of *MICPEB1c* in developing oocytes (fig. 3O and P). Detection of *MICPEB1c* expression was restricted to the ovary, which shows parallels to what is observed in other



**Fig. 3.** Cytoplasmic polyadenylation in the ctenophore *Mnemiopsis leidyi*. (A–E) Anatomy of *M. leidyi* reproductive structures and induced spawning. Dark-field microscopy images (A and C) and corresponding diagrams (B and D) depicting sagittal (A and B) and frontal (C and D) views of the gonadal structures positioned between the comb rows and mesoglea of *M. leidyi*. Male and female gametes are present on opposing sides along the midline of comb rows in lobate-stage *M. leidyi*. (E) Illustration depicting induction of *M. leidyi* spawning in cultures maintained in the laboratory under constant light exposure by placing in the dark for 4 h. (F–M) Bright field images representative of developmental progression of *M. leidyi* embryos (hpf, hours postfertilization). (N) Detection of developmentally regulated expression of cytoplasmic polyadenylation complex components GLD2 and CPEB, as well as the ectodermal marker *Lim-f*, by RT-PCR. (O and P) Differential Interference Contrast microscopy image of in situ hybridization samples displaying *MICPEB1c* mRNA expression in ovaries of a sexually mature cydippid (O) and in a dissected sample of a comb row with gonad (P). Abbreviations: ovary (o), comb row (cr), tentacle bulb (tb). (Q) Detection of expression of CPEB paralogs and the ectodermal marker *Lim-f* by RT-PCR in lobate-stage ctenophore comb rows containing gonadal tissue, zygotes, and cydippids. (R) PCR-based assessment of poly(A) tail length (as in [fig. 2K](#)) shows differences in 3'-end length for mRNAs of *M. leidyi* cyclin homologs at different developmental stages. Position of DNA size markers is shown on the right. Scale bars = 0.1 mm. Embryos displayed in (F–L) are ~0.2 mm in diameter.



animals ([Luitjens et al. 2000](#); [Rouhana et al. 2017](#)). Other CPEB1 paralogs were not detected in zygotes ([fig. 3N](#)) but were detected by RT-PCR in RNA extracted from dissected comb rows containing gonadal tissue from lobate-stage ctenophores ([fig. 3Q](#)). Altogether, these results indicate that maternal expression of CPEB1 orthologs is an ancestral feature that is shared across

metazoan lineages, which is consistent with the notion that regulation of gene expression by cytoplasmic polyadenylation is essential for early development in animals. *MICPEB1c* is available in the zygote to regulate maternal mRNAs in *M. leidyi*, whereas other CPEB1 orthologs may function at different stages of germline (sperm or egg) development.

Given the evidence for maternal deposition of cytoplasmic polyadenylation machinery in ctenophores, we asked whether conserved targets display changes representative of poly(A)-tail elongation during early development of *M. leidyi*. To do this, we identified homologs of cell cycle regulators present in the *M. leidyi* transcriptome using TBLASTN and designed gene-specific primers close to the end of their 3' UTR for analysis of poly(A)-tail length changes as in *N. vectensis* (fig. 2K). Using this approach, we looked for changes in electrophoretic mobility of 3'-end amplicons for four *cyclin* homologs during the earliest stages of development (fig. 3R). Amplicons of one *cyclin* homolog (identifier ML455312a) became longer during the transition from zygote to the 32-cell stage, decreased in size at 4-hpf, and were absent in cydippids 20-hpf (fig. 3R), indicating potential poly(A)-tail lengthening during the first embryonic cleavage events, followed by deadenylation and decay at later stages of development. Two other *cyclin* homologs displayed shortening as development progressed (fig. 3R). One of these (ML015751a) remained relatively unchanged throughout the first developmental stages analyzed, but decreased in size in cydippids, whereas the other (ML049317a) was shortened gradually and was undetectable in cydippids (fig. 3R). The size of amplicons from one of these *cyclin* homologs remained unchanged throughout the analysis (ML46822a). Intrigued by the potential changes in poly(A) tail length observed for ML455312a during the initial embryonic cleavages, we performed a more detailed assessment of poly(A) tail length changes that included analysis of each of the first four cleavages separately (supplementary fig. S10, Supplementary Material online). This approach revealed alternating increases and decreases in amplicon size following

each of the first three divisions (supplementary fig. S10, Supplementary Material online). To verify the identity of our amplicons, we cloned and sequenced cDNA from the zygote and two-cell embryos, which validated the genetic identity of ML455312a PCR products and revealed changes in poly(A) tail composition from an average of 15.7 in the zygote to ~32 adenosines in two-cell embryos (supplementary fig. S5, Supplementary Material online). We conclude that cytoplasmic polyadenylation of maternal transcripts takes place during the initial cleavages of *M. leidyi* embryos, and that cytoplasmic polyadenylation of *cyclin* homologs is a conserved feature in ctenophores, cnidarians, and vertebrates. Altogether, our results support the hypothesis that an ancestral network of post-transcriptional regulation via cytoplasmic polyadenylation is a ubiquitous feature of early development amongst animals (fig. 4).

## Discussion

Evans et al. (1983) reported the identification of cyclins as proteins made from maternal mRNA and destroyed after cell division. Years of research have uncovered how robust transcriptional regulation of cyclin genes drives progression between stages of the cell cycle in somatic cells across Eukarya (Morgan 1997; Lindqvist et al. 2009). Here, we provide evidence indicating that regulation of cyclins via cytoplasmic polyadenylation is a unifying theme in animal development. We postulate that generation of cyclins from a pool of stored mRNAs was an important innovation for evolution of multicellular development. Post-transcriptional regulation by cytoplasmic polyadenylation allows cells to bypass the requirement of generating new transcripts, which would impede the

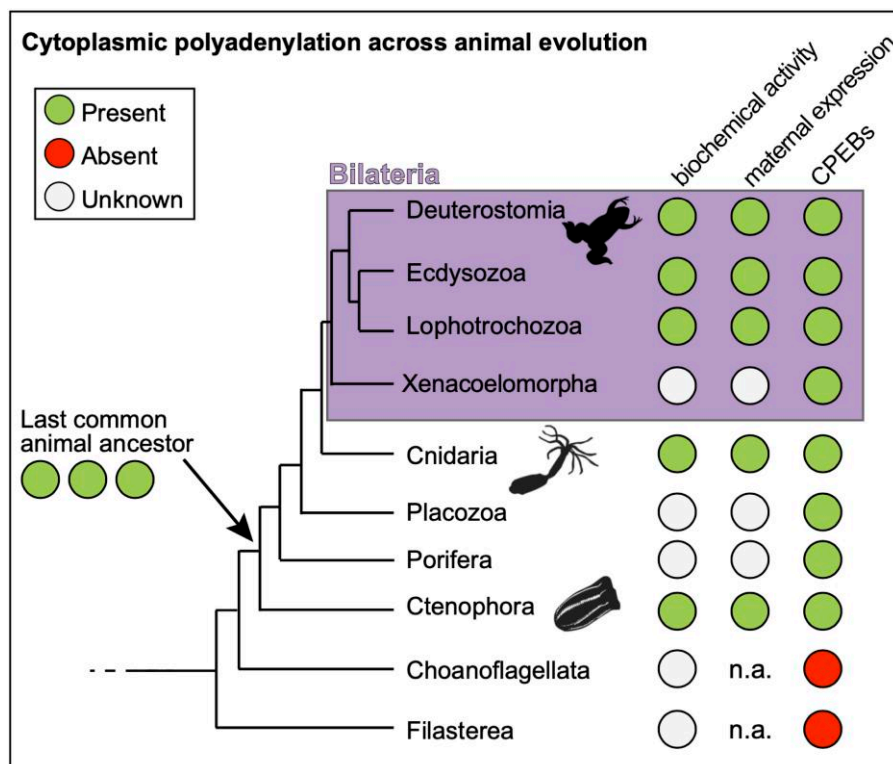


**FIG. 4.** Working model. Incorporation of results from this study with studies on bilaterians (magenta) demonstrates evidence for the presence (green circles) of CPEBs (right column) and their maternal expression (middle column) across animals. This work also demonstrates cytoplasmic polyadenylation of conserved targets across animal evolution (left column). The absence (red circle) of CPEBs in genomes of choanoflagellates and Filasterea indicates that cytoplasmic polyadenylation arose in the stem lineage of animals. White circles indicate that information is not available for a particular lineage. Animal relationships are based on Ryan et al. (2013). Abbreviation: not applicable, n.a.

quick S- to M-phase transitions observed in early embryonic development. In the absence of the ability to turn maternal mRNAs off and on, rapid mitotic divisions would have to pause between stages to allow for novel transcription to occur, bringing along large changes in gene activation programs. The enzymatic extension of poly(A) tails provides a mechanism for tunable and sequential activation of different groups of maternal mRNAs, as observed during progression from oocyte to egg to embryo (Sheets et al. 1994; Groisman et al. 2002; Pique et al. 2008; Weill et al. 2017).

### Origin of CPEBs

This study reveals the presence of CPEB1 and CPEB2 orthologs in every major animal lineage and provides evidence for cytoplasmic polyadenylation of maternal mRNAs in ctenophores and cnidarians. Whereas genetic and biochemical perturbations are necessary to conclusively determine the involvement of CPEB in cytoplasmic polyadenylation of maternal mRNAs in *M. leidyi* and *N. vectensis*, the timing of detection of cytoplasmic polyadenylation machinery and poly(A) extension of conserved targets during early development strongly parallels to what is known about function of CPEB in bilaterians. Unlike other essential components of the cytoplasmic polyadenylation machinery, such as noncanonical poly(A) polymerases of the GLD2 family (Kwak et al. 2004; Kwak and Wickens 2007; Preston et al. 2019) and subunits of the CPSF, clear CPEB orthologs are only present in metazoans. Indeed, we did not find CPEBs in Filasterea or in choanoflagellates, the latter of which are by many measures the closest relatives to animals (Lang et al. 2002; Medina et al. 2003). Given their absence in nonanimal life forms, as well as their conserved function during the transition from oocyte to zygote to multicellular embryo, we postulate that emergence of CPEBs may have been a pivotal factor in evolution of multicellular development from single celled animal ancestors.

Interestingly, the closest CPEB relatives in animals include post-transcriptional regulators of meiosis and early development, such as Musashi, Squid, Hrb27C, and DAZAP1. Both Musashi and DAZL work with CPEB to coordinate timely translation of maternal mRNAs in vertebrates (Charlesworth et al. 2006; Rutledge et al. 2014; Sousa Martins et al. 2016; Weill et al. 2017), whereas Squid and Hrb27C cooperate to regulate mRNA localization and translation in *Drosophila* oocytes (Goodrich et al. 2004; Clouse et al. 2008). These RNA-binding proteins may have coevolved to modulate the identity of their targets, as well as the timing and strength of translational activation/repression in specific animal lineages, whereas maintaining a “core” network of shared targets. Our phylogenetic analysis of RRM groups the closest nonanimal relatives of CPEB with HnRNPs present in fungi, plants, and choanoflagellates (fig. 1C). The functions of many of these proteins remain to be characterized, but the yeast protein that is most similar to CPEBs (Hrp1) is known to participate in transcriptional termination and 3'-end processing, as well as to shuttle between the nucleus and the

cytoplasm, and mark messages for nonsense-mediated decay (Kessler et al. 1997; Minvielle-Sebastia et al. 1998; Gonzalez et al. 2000). Characterization of more members of this group of RRM-containing proteins will be needed to form a formal hypothesis regarding the origin of CPEBs. One possibility is that CPEBs derived from ancestral nuclear HnRNPs that participate in 3'-end processing and maintained interactions with CPSF.

### Ancestral CPEB Architecture

High primary sequence conservation is found in the C-terminal region across CPEB orthologs (40–90%) and paralogs (>30%), with highest identity being shared amongst CPEB2 subfamily members (Rouhana et al. 2017; Hervás et al. 2021). This can be predicted to reflect not only strong selection for the specificity of RNA binding provided by RRMs that reside in this region of the protein but also of its participation in conserved protein–protein interactions. For example, the Zinc-Finger domain at the end of the RBD of CPEBs is predicted to bind sumoylated proteins required for cytoplasmic polyadenylation, such as CPSF and the scaffolding protein Symplekin (Barnard et al. 2004; Merkel et al. 2013). Surprisingly, not all CPEB partners interact with the conserved region of the protein. For example, members of the PUF family of proteins work with CPEBs to maintain repression of target mRNAs in nematodes, flies, and vertebrates (Nakahata et al. 2001; Campbell et al. 2012). Physical association between the CPEB protein CPB-1 and the PUF family member FBF-1 from *C. elegans* was mapped to a small motif that resides in a disordered region upstream of the RBD (Menichelli et al. 2013). In addition, motifs for phosphorylation and ubiquitination of CPEB, which modulate regulated timing of activation of cytoplasmic polyadenylation and destruction of CPEB (respectively), also reside outside of the conserved RBD (Mendez, Hake, et al. 2000; Mendez, Murthy, et al. 2000; Hodgman et al. 2001; Setoyama et al. 2007). Nevertheless, sequence conservation outside of the RBD of CPEBs from different phyla is not prevalent, and this may reflect highly specific needs for regulation of CPEB activity in each species or limitations in our programs for sequence analysis.

One domain that has been characterized in the N-terminal region of some CPEBs is stretches of glutamine-rich sequence that mediate prion-like conformational changes (Si, Lindquist, et al. 2003; Majumdar et al. 2012; Raveendra et al. 2013; Hervás et al. 2021). Although their position and presence across orthologs are not conserved, stretches of polyglutamine in CPEB orthologs from *Drosophila* and the marine snail *Aplysia* are required for proper memory formation (Si, Lindquist, et al. 2003; Fioriti et al. 2015; Oroz et al. 2020) reviewed by Si and Kandel (2016). Whereas the *Aplysia* protein originally found to form prions is a CPEB1 ortholog, prion domains are found in CPEB2 subfamily members in mammals, planarians, and flies. Amongst ctenophores, putative prion domains are present in *M. leidyi* CPEB1a and a CPEB1 paralog in *B. ovata* (supplementary table S3, Supplementary Material online). Furthermore, we identified putative prion domains in

both CPEB1 and CPEB2 orthologs in the ctenophore *H. californensis* (supplementary table S3, Supplementary Material online). The presence of prion domains in CPEBs across major animal lineages suggests that prion-mediated aggregation may be a shared characteristic that facilitates some contribution(s) that cytoplasmic polyadenylation brings to animal biology. However, the distribution of prion domains suggests that these may be products of convergent evolution. It will be interesting to see whether some CPEBs utilize prion conformation to form aggregates of ribonucleoprotein in the germline, as thus far is known to occur in neurons.

### Correlation Between Length of Poly(A) Tail and mRNA Stability or Translation

The poly(A) tail of an mRNA protects the 3'-end of the message from degradation and promotes translational efficiency (Goldstrohm and Wickens 2008; Roy and Jacobson 2013). Benefits bestowed by the poly(A) tail are mediated by cytoplasmic poly(A)-binding proteins (PABPCs), which bind to poly(A) every 27 residues upon mRNA export into the cytoplasm (Baer and Kornberg 1980; Jacobson 1996; Jacobson and Peltz 1996; Mangus et al. 2003). PABPCs can also bind translation initiation factors attached to the 5'-cap, forming a bridge between both ends of the message and arranging mRNAs into "closed-loop" structures that are believed to support the stability and recycling of ribosomes (Jacobson 1996; Sachs and Varani 2000). Poly(A)-binding proteins can also directly stimulate translational initiation *in trans* (Kahvejian et al. 2005), or when tethered to a message (Coller et al. 1998; Gray et al. 2000), regardless of the presence of a poly(A) tail.

Recent studies have shown that the correlation between poly(A) tail length and translational efficiency is absent in somatic cells and lost after zygotic genome activation (Subtelny et al. 2014; Park et al. 2016; Lima et al. 2017). One explanation for the uncoupling between poly(A) tail length and translational efficiency is that levels of PABPCs are rate-limiting in the oocyte but increase later in development (Xiang and Bartel 2021). An alternative hypothesis, although not mutually exclusive from the one aforementioned, is that multiple units of PABPC must be bound to an mRNA for translational stimulation. A minimum of 12 adenosines is required for poly(A)-binding protein and multiples of 27 for assembly of multiple units (Baer and Kornberg 1980, 1983; Sachs et al. 1986). However, this second hypothesis is challenged by the observation that the correlation between poly(A) tail length and translational efficiency is lost after the ~20 nucleotide threshold in HeLa cells, which suggests that binding by one PABPC may be enough for translational stimulation (Park et al. 2016), as well as by the observation that repressed *c-mos* and *cyclinB1* mRNAs have an average length of 50 and 30 adenosines (respectively) when repressed in *Xenopus* oocytes (Sheets et al. 1994). A third hypothesis posits that the type and combinations of PABPCs in specific cell types lead to different dynamics

between poly(A) tail length and translational efficiency (Wigington et al. 2014).

Whereas further studies are needed to measure the precise length of poly(A) tails in ctenophores and cnidarians, it is worth considering the observation that tails of repressed cytoplasmic polyadenylation targets in *N. vectensis* may be shorter than the minimal requirement for binding a single PABPC (fig. 2M–O; supplementary file S2; supplementary figs. S5 and S6, Supplementary Material online). This observation suggests that either PABPC binding is dispensable for protection from mRNA decay in oocytes and eggs of *N. vectensis*, or that PABPC binding has a smaller footprint in these species. Indeed, NanoLuc reporter mRNAs lacking a poly(A) tail were as stable as polyadenylated counterparts in injected *N. vectensis* eggs (supplementary fig. S3D, Supplementary Material online). Conversely, the polyadenylated status for conserved CPEB substrates in *Nematostella* yielded tails that sometimes surpassed the 100-nucleotide mark (fig. 2L and O), whereas lengthening of the poly(A) tail in *Mnemiopsis* was much more modest (albeit sampling the latter is limited to one cyclin gene; figs. 3R and S10, Supplementary Material online). Future global surveys of poly(A) dynamics during development will lead to an understanding of whether shorter poly(A) tails are the norm in *M. leidyi*, and the degree to which translational enhancement is provided by small increments (20–30 nucleotides) in poly(A) tail length in ctenophores and cnidarians.

### Composition of mRNA Tails

The GLD-2 family is composed of ribonucleotidyl transferases that synthesize poly(A), but it also includes poly(U) polymerases (a.k.a. TUTases), poly(A) polymerases that incorporate intermittent guanosines within the poly(A) tail, and even polymerases that generate tails of (GU) repeats (Kwak et al. 2004; Kwak and Wickens 2007; Modepalli and Moran 2017; Preston et al. 2019). Whereas oligouridylation by TUTases marks RNAs for degradation (Shen and Goodman 2004; Lim et al. 2014; Meaux et al. 2018), the description of mixed tailing in the literature remains relatively novel and scarce in comparison. Recently, detection of poly(UG) tails was reported in targets of RNA-interference and transposons in *C. elegans*, where they serve as template for RNA-dependent RNA polymerase synthesis of trans-generational siRNAs (Shukla et al. 2020). Intermittent incorporation of guanosine in the poly(A) tail has recently been shown to stall deadenylation machinery and prolong the life of specific maternal mRNAs in zebrafish and *Xenopus* embryos (Lim et al. 2018). TENT4 proteins are the enzymes responsible for intermittent guanylation (Lim et al. 2018), but intermittent guanosines are also deposited by GLD2 (i.e., TENT2) orthologs when tethered to reporter RNAs (Kwak and Wickens 2007). We observed intermittent guanosines in poly(A) tails of maternal mRNA from *N. vectensis*, suggesting that this feature of tail regulation may also be ancestral to bilaterians and cnidarians, and may result from enzymes with lower fidelity than nuclear poly(A) polymerases.

Uridylation at the 3'-end of short poly(A) tails has been observed in animals, plants, and fungi (Morozov et al. 2012; Sement et al. 2013; Chang et al. 2014). We observed instances of non-templated uridines at the start of some analyzed mRNA tails from *N. vectensis*. However, clear differences in prevalence and position of uridine within the tail were observed between sequencing approaches (supplementary figs. S5–S8, Supplementary Material online). When using Amplicon-EZ sequencing, oligouridine was observed at the first positions of the tail almost as often as adenine and decreasing in prevalence downstream (supplementary fig. S6C–E and supplementary file S2, Supplementary Material online). Similar observations were reported for *cyclinB* mRNA in starfish oocytes, where oligouridine present at the initial positions of the tail was slightly trimmed during meiotic progression and cytoplasmic polyadenylation (Ochi and Chiba 2016). Uridines at the start of the tail do not seem to be conducive to decay in the oocyte or the egg and remain present even after cytoplasmic polyadenylation (Ochi and Chiba 2016). Ochi and Chiba hypothesized that oligouridine at the start of the tail may be involved in translational inactivation of mRNAs. Another possibility is that runs of uridine present at the start of the tail serve as a pre-existing mark to accelerate decay, and these become functional after deadenylation and the activation of mRNA degradation machinery during the maternal-to-zygotic transition (Walser and Lipshitz 2011). Further studies will be needed to determine the pervasiveness of this structure on maternal transcripts of different animal species, as well as the identity of the polymerase responsible for incorporating uridine at beginning positions of the tail.

## Materials and Methods

### Reproducibility and Transparency Statement

Custom scripts, command lines, and data used in these analyses, including sequencing reads, as well as alignments and tree files, are available at [https://github.com/lrouhana/cpeb\\_evolution](https://github.com/lrouhana/cpeb_evolution). To maximize transparency and minimize confirmation bias, we planned analyses a priori using phylotool (DeBiase and Ryan 2019) and posted this original document and any subsequent changes to our GitHub repository (URL above).

### Identification and Phylogenetic Analyses of CPEBs

We identified putative CPEBs and outgroup sequences with the following approach. We used BLASTP version 2.10.1 with the query sequence Human CPEB1 (NP\_001275748) against a database that included protein models from the following species: *S. cerevisiae*, *S. pombe*, *A. thaliana*, *C. owczarzaki*, *S. rosetta*, *A. queenslandica*, *N. vectensis*, *T. adhaerens*, *D. melanogaster*, *C. teleta*, *M. musculus*, *D. rerio*, and *M. leidyi*. We also ran the same BLASTP using the web interface at PlanMine version 3.0

(Rozanski et al. 2019) to identify CPEBs and related sequences from *S. mediterranea*.

We downloaded hidden Markov models (HMMs) from PFAM as follows: RRM\_1 (PF00076), RRM\_7 (PF16367), and CEBP\_ZZ (PF16366). For CEBP\_ZZ, which should only occur once per CPEB protein, we created an alignment of CEBP\_ZZ domains using *hmm2aln.pl* version 0.05 (<https://github.com/josephryan/hmm2aln.pl>), which uses *hmmsearch* from HMMer version 3.3 (Potter et al. 2018) to identify target domains in protein sequences and construct an alignment to the query hidden Markov model. For the RRM\_1 and RRM\_7 HMMs, which often produce overlapping results, we ran *hmmsearch* separately with each of these HMMs and merged overlapping results by taking the lowest N-terminal coordinate and the highest C-terminal coordinate from the two results. We extracted the amino acid sequences between the start and end of the match and used MAFFT version 7.407 (Katoh and Frith 2012) with default parameters to generate an alignment of RNA recognition motifs (RRMs). We used IQ-TREE version 1.6.12 (Nguyen et al. 2015) with default parameters to generate a maximum-likelihood tree from all resulting alignments. All command lines, scripts, and sequence sources used in this section are available in our GitHub repository ([https://github.com/lrouhana/cpeb\\_evolution](https://github.com/lrouhana/cpeb_evolution)). We used a web interface to perform reciprocal best Blast searches to identify CPEBs in *B. ovata* and *H. californensis* (see supplementary table S2, Supplementary Material online).

### Husbandry and Spawning of Animals in the Laboratory

Husbandry of laboratory lines of *N. vectensis* was performed as per Wijesena et al. (2017). Briefly, separate *N. vectensis* male and female colonies were maintained in separate bowls at 17 °C in one-third seawater under dark conditions and fed freshly hatched *Artemia* 1–2 times per week. We induced spawning of sexually mature animals by overnight exposure increased temperature and light as described by Hand and Uhlinger (1992) following ingestion of minced oyster 24–48 h prior. Upon spawning, eggs were dejellied using 3% cysteine solution in one-third seawater (pH ~7.5), fertilized and/or injected with reporter mRNAs, and collected for RNA extraction in TRI Reagent (Sigma-Aldrich, St. Louis, MO). Injections and development of fertilized eggs were performed in one-third filtered seawater at room temperature as described by Layden et al. (2013).

We collected *M. leidyi* hermaphrodites from floating docks on waters surrounding the Whitney Laboratory of Marine Biosciences, Marineland, FL, and maintained them as per Ramon-Mateu et al. (2022). We induced spawning by interrupting continuous light exposure for ~4 h as per Pang and Martindale (2008), then visualized embryos under light microscopy and collected at the

desired stages manually to freeze immediately at  $-80^{\circ}\text{C}$  in TRI Reagent for RNA extraction.

### Generation of cDNA and Assessment of Gene Expression by RT-PCR

Total RNA was extracted from *N. vectensis* ovaries, or groups of 20 eggs, embryos, and polyps using TRI Reagent as per manufacturer's instructions (Sigma-Aldrich, St. Louis, MO) and resuspended in 8  $\mu\text{l}$  of RNase-free water. One microgram of total RNA was then ligated to 0.4  $\mu\text{g}$  of GB135 3'-amino-modified DNA anchor primer (table 1) as per Rassa et al. (2000) and Charlesworth et al. (2004), using T4 RNA ligase (New England Biolabs, Ipswich, MA) in 10- $\mu\text{l}$  volume reactions. After 2-h incubation at  $25^{\circ}\text{C}$ , and heat inactivation of T4 RNA ligase through 15 min of incubation at  $65^{\circ}\text{C}$ , the contents of the ligation reaction were used as input for reverse transcription. The 50- $\mu\text{l}$  SuperScript IV Reverse Transcription reactions were performed as per the manufacturer's instructions (Invitrogen, Carlsbad, CA), using the entire volume of corresponding T4 RNA ligation reaction and 0.5  $\mu\text{g}$  of GB136\_T5 primer (table 1). The reverse transcription reaction was heat inactivated by incubation at  $85^{\circ}\text{C}$  for 5 min. Then, 1- $\mu\text{l}$  volumes of Reverse Transcription reactions were used as template for amplification of internal cDNA fragments using in 20- $\mu\text{l}$  volume PCR reactions (35 rounds of amplification using Promega 2X PCR Master Mix (Promega, Madison, WI). Gene-specific primers and annealing temperatures are listed in table 1. The identity of PCR products was verified by Sanger sequencing of amplicons cloned using the pGEM-T cloning system (Promega, Madison, WI) as per manufacturer's instructions.

*Mnemiopsis leidyi* cDNA synthesis was performed as described above, but RNA was extracted from groups of 50 embryos or cydippids and resuspended in 6  $\mu\text{l}$  of RNase-free water. Five microliters from the total resuspension were used as input for ligation with GB135 oligo using T4 RNA ligase. The following steps proceeded as detailed above using the primers and annealing temperatures listed in table 1. For analysis of CPEB paralog expression in comb rows containing gonadal tissue dissected from lobate-stage *M. leidyi*, reverse transcription was performed using Promega's GoTaq 2-Step system with oligo(dT) and randomized primers as per manufacturer's instructions (Promega, Madison, WI).

### Poly(A)-tail Length Assays

cDNAs generated using the GB135 adapter as described above were used as templates for amplification and analysis of poly(A) tail length as per Charlesworth et al. (2004) and Rouhana and Wickens (2007) with slight modifications. Briefly, 2  $\mu\text{l}$  of reverse transcription reaction was used directly as template for amplification of 3'-ends using the GB136-T5 primer and a gene-specific primer (See table 1 for utilized primers and annealing temperatures). Gene-specific primers were designed to target sequence within  $\sim 150$  nucleotides from the furthest cleavage and polyadenylation site for each gene according to predicted

gene models, EST reads, and RNAseq reads available for *N. vectensis* (<https://mycocosm.jgi.doe.gov/Nemve1/Nemve1.home.html> (Putnam et al. 2007); <https://genomes.stowers.org/starletseanemone> (Zimmermann et al. 2022)) and *M. leidyi* predicted transcripts (<https://research.nhgri.nih.gov/mnemiopsis/>; Ryan et al. 2013; Moreland et al. 2014; Moreland et al. 2020). A total of 5  $\mu\text{l}$  of product from 35 rounds of PCR was analyzed for each timepoint in by 2% agarose gel electrophoresis (Top Vision, Thermo Scientific, Waltham, MA). Each result is representative of a minimum of two independent replicates.

For generation of 3'-end PCR products used in Amplicon-EZ sequencing, cDNA was synthesized as described above, and 3  $\mu\text{l}$  of reverse transcription reaction was used as template for 35 rounds of amplification using *Nv\_cyclin1*, *Nv\_cyclin3*, and *Nv\_c-mos* forward primers with partial Illumina adapter sequence on their 5'-end, as well as primers including the GB-136T5 oligo sequence with a second Illumina adapter sequence, as recommended by the sequencing service provider (Genewiz, South Plainfield, NJ; see table 1). Amplicons were purified using DNA Clean & Concentrator-5 columns (Zymo Research, Irvine, CA), eluted in water, diluted to a concentration of 20 ng/ $\mu\text{L}$ , and shipped for sequencing.

### Computation Analyses of Poly(A)-tail Sequencing Amplicon-EZ Data

We used NGmerge version 0.3 (Gaspar 2018) to merge overlapping paired-end sequences and correct erroneous and ambiguous base calls in our resulting poly(A)-tail sequencing data. We retained only those merged sequences that contained the 19-bp linker sequence. We masked the linker sequences and then applied a k-mer strategy ( $k = 20$ ) to mask UTR sequence present in the merged sequences. We considered poly(A) tails to be the bases between the masked UTR and linker sequences and calculated statistical data (e.g., composition, mean, and median lengths) from these predicted tails. All command lines and scripts used to identify tails and compute statistics are available in our GitHub repository ([https://github.com/lrouhana/cpeb\\_evolution](https://github.com/lrouhana/cpeb_evolution)).

### Direct Sequencing of *N. vectensis* mRNAs Using Oxford Nanopore Technology

An mRNA library was created using Nanopore's direct RNA sequencing kit (SQK-RNA002) from extracted total RNA of unfertilized *N. vectensis* eggs per the manufacturer's recommended instructions (Oxford Nanopore Technologies, Oxford, United Kingdom). Sequencing was performed using the minION device. Base calling and quality control of minION's .fast5 files were performed using default parameters on guppy. The resulting .fastq files were compiled into a reference .fasta file (supplementary file S3, Supplementary Material online), which was used to identify relevant reads via BlastN, which were later aligned to the reference cDNAs in CLC workbench.

## Translational Assessment of Injected Luciferase Reporter mRNAs Using *N. vectensis*

Firefly luciferase and NanoLuc luciferase mRNAs were generated from pT7-Luc and pT7-Nanoluc vectors templates (Sheets 2019) using the mMessage mMachine T7 Ultra transcription kit (Invitrogen, Waltham, MA). Templates were linearized with BglII and cleaned up using DNA Clean & Concentrator-5 columns (Zymo Research, Irvine, CA). For polyadenylated mRNAs, recombinant yeast Poly(A) Polymerase (PAP) from the mMessage mMachine T7 Ultra transcription kit was used on half of the in vitro transcribed mRNAs, the other half was left without a poly(A) tail for comparison. After testing serial dilutions of mRNA concentrations (supplementary fig. S3, Supplementary Material online) it was decided to co-inject Nanoluc mRNAs ( $\pm p(A_{\sim 350})$ ) with luciferase mRNAs ( $p(A_0)$ ) as loading controls at a concentration of 25 ng/ $\mu$ l (each) into dejellied *N. vectensis* eggs and zygotes as per Layden et al. (2013). Nanoluc and luciferase signals were measured in 96-well plates, from four groups of five eggs or embryos, 6 h postinjection using a Synergy HTX Multi-mode Microplate Reader (Bio Tek Instruments, Winooski, VT) and the Nano-Glo Dual Luciferase Reporter System (Promega, Madison, WI) as per the manufacturer's instructions. Luminescence from NanoLuc reporter was normalized to co-injected firefly luciferase signal, and the average ratio of normalized NanoLuc signals was compared between groups of samples injected with polyadenylated and non-polyadenylated Nanoluc mRNAs. Levels of reporter mRNAs in eggs were measured 6 h postinjection by RT-qPCR using the GoTaq 2-Step RT-qPCR system as per manufacturer's instructions (Promega, Madison, WI) with random primers for reverse transcription and oligos listed in table 1 for the qPCR step.

## Analysis of *MICPEB1c* Expression by In Situ Hybridization

Partial *MICPEB1c* (ML05854a) sequence was amplified from *M. leidyi* cDNA using primers listed in table 1. Amplicons were cloned into the pGEM-T vector (Promega, USA) and their identity confirmed using Sanger sequencing. Riboprobes labeled with digoxigenin (DIG) were generated using this construct as template for in vitro transcription (Megascript SP6 transcription kit, Invitrogen, Waltham, MA) and diluted into a 1 ng/ $\mu$ l-stock working solution in hybridization buffer. *M. leidyi* cydippids with visible gonads and not fed 1 day prior were fixed as previously described and stored in methanol until their use for in situ hybridization as per Mitchell et al. (2021).

## Supplementary Material

Supplementary data are available at *Molecular Biology and Evolution* online.

## Acknowledgments

We gratefully acknowledge the Sunset Inlet Homeowners Association in Beverly Beach and Marker 8 Hotel and

Marina in St. Augustine for facilitating the animal collections on their properties. We thank current and former members of the Martindale laboratory, in particular, Leslie Babonis, Radim Zidek, Brent Foster, Dorothy Mitchell, and Camille Enjolras, for the technical advice and assistance during completion of this project. We would also like to thank Sandra Loesgen for the generous access to lab equipment. Research reported in this publication was supported by The Eunice Kennedy Shriver National Institute of Child Health and Human Development of the National Institutes of Health (R15HD082754) to L.R., an Allen Distinguished Investigator Award and a Paul G. Allen Frontiers Group advised grant of the Paul G. Allen Family Foundation to J.F.R. and M.Q.M, as well as grants from the National Science Foundation (IOS-1755364) and the National Aeronautics and Space Administration (80NSSC18K1067) to M.Q.M. A.E. was supported by a National Science Foundation Postdoctoral Research Fellowship in Biology (DBI-2010755). Contributions by V.D. were supported by the Nancy Goranson Endowment and a Teaching Assistantship provided by the Office of Graduate Studies at UMass Boston. The funders had no role in study design, data collection and analysis, decision to publish, or preparation of the manuscript.

## Data Availability

Custom scripts, command lines, and data used in these analyses, including Amplicon-EZ sequencing reads, as well as alignments and tree files, are available at [https://github.com/lrouhana/cpeb\\_evolution](https://github.com/lrouhana/cpeb_evolution). Illumina RNA-sequencing and Nanopore Direct RNA sequencing reads are available at NCBI under BioProject IDs PRJNA893363 and PRJNA956458, respectively. Records of cloned cDNA fragments were deposited in NCBI under GenBank accession numbers OP806308-OP806311 and OP852652-OP852653.

## Author Contributions

L.R. directed the overall framework of the project and performed molecular analyses and injection of mRNAs; A.E. contributed RNAseq reads from *Nematostella* and anatomical analyses of *Mnemiopsis*, F.H. performed in situ hybridization analysis in *Mnemiopsis*, V.D. performed Nanopore Direct RNA sequencing and analysis, and J.F.R. developed programs and performed bioinformatic and phylogenetic analyses; M.Q.M. provided organisms for molecular studies and performed injection of mRNAs; and L.R., A.E., F.H., M.Q.M., and J.F.R. contributed to preparation of the manuscript.

## References

- Afroz T, Skrisovska L, Belloc E, Guillen-Boixet J, Mendez R, Allain FH-T. 2014. A fly trap mechanism provides sequence-specific RNA recognition by CPEB proteins. *Genes Dev.* **28**:1498–1514.
- Bachvarova RF. 1992. A maternal tail of poly(A): the long and the short of it. *Cell* **69**:895–897.

- Baer BW, Kornberg RD. 1980. Repeating structure of cytoplasmic poly(A)-ribonucleoprotein. *Proc Natl Acad Sci U S A*. **77**: 1890–1892.
- Baer BW, Kornberg RD. 1983. The protein responsible for the repeating structure of cytoplasmic poly(A)-ribonucleoprotein. *J Cell Biol*. **96**:717–721.
- Barkoff A, Ballantyne S, Wickens M. 1998. Meiotic maturation in *Xenopus* requires polyadenylation of multiple mRNAs. *EMBO J*. **17**:3168–3175.
- Barnard DC, Ryan K, Manley JL, Richter JD. 2004. Symplekin and xGLD-2 are required for CPEB-mediated cytoplasmic polyadenylation. *Cell*. **119**:641–651.
- Barr J, Gilmudtinov R, Wang L, Shidlovskii Y, Schedl P. 2019. The *Drosophila* CPEB protein orb specifies oocyte fate by a 3' UTR-dependent autoregulatory loop. *Genetics*. **213**:1431–1446.
- Benoit P, Papin C, Kwak JE, Wickens M, Simonelig M. 2008. PAP- and GLD-2-type poly(A) polymerases are required sequentially in cytoplasmic polyadenylation and oogenesis in *Drosophila*. *Development*. **135**:1969–1979.
- Bilger A, Fox CA, Wahle E, Wickens M. 1994. Nuclear polyadenylation factors recognize cytoplasmic polyadenylation elements. *Genes Dev*. **8**:1106–1116.
- Brachet J, Ficq A, Tencer R. 1963. Amino acid incorporation into proteins of nucleate and anucleate fragments of sea urchin eggs: effect of parthenogenetic activation. *Exp Cell Res*. **32**:168–170.
- Calderone V, Gallego J, Fernandez-Miranda G, Garcia-Pras E, Maillou C, Berzigotti A, Mejias M, Bava FA, Angulo-Urarte A, Graupera M, et al. 2016. Sequential functions of CPEB1 and CPEB4 regulate pathologic expression of vascular endothelial growth factor and angiogenesis in chronic liver disease. *Gastroenterology*. **150**: 982–997.e30.
- Campbell ZT, Menichelli E, Friend K, Wu J, Kimble J, Williamson JR, Wickens M. 2012. Identification of a conserved interface between PUF and CPEB proteins. *J Biol Chem*. **287**:18854–18862.
- Chang H, Lim J, Ha M, Kim VN. 2014. TAIL-seq: genome-wide determination of poly(A) tail length and 3' end modifications. *Mol Cell*. **53**:1044–1052.
- Chang JS, Tan L, Wolf MR, Schedl P. 2001. Functioning of the *Drosophila* orb gene in *gurken* mRNA localization and translation. *Development*. **128**:3169–3177.
- Chao H-W, Tsai L-Y, Lu Y-L, Lin P-Y, Huang W-H, Chou H-J, Lu W-H, Lin H-C, Lee P-T, Huang Y-S. 2013. Deletion of CPEB3 enhances hippocampus-dependent memory via increasing expressions of PSD95 and NMDA receptors. *J Neurosci*. **33**:17008–17022.
- Charlesworth A, Cox LL, MacNicol AM. 2004. Cytoplasmic polyadenylation element (CPE)- and CPE-binding protein (CPEB)-independent mechanisms regulate early class maternal mRNA translational activation in *Xenopus* oocytes. *J Biol Chem*. **279**:17650–17659.
- Charlesworth A, Meijer HA, de Moor CH. 2013. Specificity factors in cytoplasmic polyadenylation. *Wiley Interdiscip Rev RNA*. **4**: 437–461.
- Charlesworth A, Wilczynska A, Thampi P, Cox LL, MacNicol AM. 2006. Musashi regulates the temporal order of mRNA translation during *Xenopus* oocyte maturation. *EMBO J*. **25**:2792–2801.
- Chen P-J, Huang Y-S. 2012. CPEB2–eEF2 interaction impedes HIF-1 $\alpha$  RNA translation. *EMBO J*. **31**:959–971.
- Chen J, Melton C, Suh N, Oh JS, Horner K, Xie F, Sette C, Billeloch R, Conti M. 2011. Genome-wide analysis of translation reveals a critical role for deleted in azoospermia-like (Dazl) at the oocyte-to-zygote transition. *Genes Dev*. **25**:755–766.
- Christerson LB, McKearin DM. 1994. Orb is required for anteroposterior and dorsoventral patterning during *Drosophila* oogenesis. *Genes Dev*. **8**:614–628.
- Clouse KN, Ferguson SB, Schupbach T. 2008. Squid, Cup, and PABP55B function together to regulate *gurken* translation in *Drosophila*. *Dev Biol*. **313**:713–724.
- Coller JM, Gray NK, Wickens MP. 1998. mRNA stabilization by poly(A) binding protein is independent of poly(A) and requires translation. *Genes Dev*. **12**:3226–3235.
- Crittenden SL, Eckmann CR, Wang L, Bernstein DS, Wickens M, Kimble J. 2003. Regulation of the mitosis/meiosis decision in the *Caenorhabditis elegans* germline. *Philos Trans R Soc Lond B Biol Sci*. **358**:1359–1362.
- Crooks GE, Hon G, Chandonia JM, Brenner SE. 2004. Weblogo: a sequence logo generator. *Genome Res*. **14**:1188–1190.
- Cui J, Sackton KL, Horner VL, Kumar KE, Wolfner MF. 2008. Wispy, the *Drosophila* homolog of GLD-2, is required during oogenesis and egg activation. *Genetics*. **178**:2017–2029.
- Curtis D, Lehmann R, Zamore PD. 1995. Translational regulation in development. *Cell*. **81**:171–178.
- Dai T, Vera Y, Salido EC, Yen PH. 2001. Characterization of the mouse Dazap1 gene encoding an RNA-binding protein that interacts with infertility factors DAZ and DAZL. *BMC Genomics*. **2**:6.
- Darnell JC, Richter JD. 2012. Cytoplasmic RNA-binding proteins and the control of complex brain function. *Cold Spring Harb Perspect Biol*. **4**:a012344.
- DeBiaise MB, Ryan JF. 2019. Phylotocol: promoting transparency and overcoming bias in phylogenetics. *Syst Biol*. **68**:672–678.
- de Moor CH, Meijer H, Lissenden S. 2005. Mechanisms of translational control by the 3' UTR in development and differentiation. *Semin Cell Dev Biol*. **16**:49–58.
- de Moor CH, Richter JD. 1999. Cytoplasmic polyadenylation elements mediate masking and unmasking of cyclin B1 mRNA. *EMBO J*. **18**:2294–2303.
- Dickson KS, Bilger A, Ballantyne S, Wickens MP. 1999. The cleavage and polyadenylation specificity factor in *Xenopus laevis* oocytes is a cytoplasmic factor involved in regulated polyadenylation. *Mol Cell Biol*. **19**:5707–5717.
- Dominski Z, Marzluff WF. 2007. Formation of the 3' end of histone mRNA: getting closer to the end. *Gene*. **396**:373–390.
- Dreyfuss G. 1986. Structure and function of nuclear and cytoplasmic ribonucleoprotein particles. *Annu Rev Cell Biol*. **2**:459–498.
- Duran-Arque B, Canete M, Castellazzi CL, Bartomeu A, Ferrer-Caelles A, Reina O, Caballe A, Gay M, Arauz-Garofalo G, Belloc E, et al. 2022. Comparative analyses of vertebrate CPEB proteins define two subfamilies with coordinated yet distinct functions in post-transcriptional gene regulation. *Genome Biol*. **23**:192.
- Evans T, Rosenthal ET, Youngblom J, Distel D, Hunt T. 1983. Cyclin: a protein specified by maternal mRNA in sea urchin eggs that is destroyed at each cleavage division. *Cell*. **33**:389–396.
- Fernandez-Miranda G, Mendez R. 2012. The CPEB-family of proteins, translational control in senescence and cancer. *Ageing Res Rev*. **11**:460–472.
- Fioriti L, Myers C, Huang Y-Y, Li X, Stephan JS, Trifileff P, Colnaghi L, Kosmidis S, Drisaldi B, Pavlopoulos E, et al. 2015. The persistence of hippocampal-based memory requires protein synthesis mediated by the prion-like protein CPEB3. *Neuron*. **86**: 1433–1448.
- Fischer AH, Pang K, Henry JQ, Martindale MQ. 2014. A cleavage clock regulates features of lineage-specific differentiation in the development of a basal branching metazoan, the ctenophore *Mnemiopsis leidyi*. *Evodevo*. **5**:4.
- Fox CA, Sheets MD, Wickens MP. 1989. Poly(A) addition during maturation of frog oocytes: distinct nuclear and cytoplasmic activities and regulation by the sequence UUUUUU. *Genes Dev*. **3**: 2151–2162.
- Gaspar JM. 2018. NGmerge: merging paired-end reads via novel empirically-derived models of sequencing errors. *BMC Bioinformatics*. **19**:536.
- Geuens T, Bouhy D, Timmerman V. 2016. The hnRNP family: insights into their role in health and disease. *Hum Genet*. **135**:851–867.
- Giagarra V, Igea A, Castellazzi CL, Bava FA, Mendez R. 2015. Global analysis of CPEBs reveals sequential and non-redundant functions in mitotic cell cycle. *PLoS One*. **10**:e0138794.
- Goldstrohm AC, Wickens M. 2008. Multifunctional deadenylase complexes diversify mRNA control. *Nat Rev Mol Cell Biol*. **9**: 337–344.



- Gonzalez CI, Ruiz-Echevarria MJ, Vasudevan S, Henry MF, Peltz SW. 2000. The yeast hnRNP-like protein Hrp1/Nab4 marks a transcript for nonsense-mediated mRNA decay. *Mol Cell*. **5**:489–499.
- Goodrich JS, Clouse KN, Schupbach T. 2004. Hrb27C, Sqd and Otu cooperatively regulate *gurken* RNA localization and mediate nurse cell chromosome dispersion in *Drosophila* oogenesis. *Development* **131**:1949–1958.
- Gray NK, Collier JM, Dickson KS, Wickens M. 2000. Multiple portions of poly(A)-binding protein stimulate translation in vivo. *EMBO J*. **19**:4723–4733.
- Groisman I, Jung MY, Sarkissian M, Cao Q, Richter JD. 2002. Translational control of the embryonic cell cycle. *Cell* **109**:473–483.
- Hagele S, Kuhn U, Boning M, Katschinski DM. 2009. Cytoplasmic polyadenylation-element-binding protein (CPEB)1 and 2 bind to the HIF-1 $\alpha$  mRNA 3'-UTR and modulate HIF-1 $\alpha$  protein expression. *Biochem J*. **417**:235–246.
- Hake LE, Mendez R, Richter JD. 1998. Specificity of RNA binding by CPEB: requirement for RNA recognition motifs and a novel zinc finger. *Mol Cell Biol*. **18**:685–693.
- Hake LE, Richter JD. 1997. Translational regulation of maternal mRNA. *Biochim Biophys Acta*. **1332**:M31–M38.
- Hand C, Uhlinger KR. 1992. The culture, sexual and asexual reproduction, and growth of the sea anemone *Nematostella vectensis*. *Biol Bull*. **182**:169–176.
- Harvey EB. 1936. Parthenogenetic merogony or cleavage without nuclei in *Arbacia punctulata*. *Biol Bull*. **71**:101–121.
- Hasegawa E, Karashima T, Sumiyoshi E, Yamamoto M. 2006. *C. elegans* CPB-3 interacts with DAZ-1 and functions in multiple steps of germline development. *Dev Biol*. **295**:689–699.
- Hentze MW. 1995. Translational regulation: versatile mechanisms for metabolic and developmental control. *Curr Opin Cell Biol*. **7**:393–398.
- Hervas R, Del Carmen Fernandez-Ramirez M, Galera-Prat A, Suzuki M, Nagai Y, Bruix M, Menendez M, Laurens DV, Carrion-Vazquez M. 2021. Divergent CPEB prion-like domains reveal different assembly mechanisms for a generic amyloid-like fold. *BMC Biol*. **19**:43.
- Hodgman R, Tay J, Mendez R, Richter JD. 2001. CPEB phosphorylation and cytoplasmic polyadenylation are catalyzed by the kinase IAK1/Eg2 in maturing mouse oocytes. *Development* **128**:2815–2822.
- Huang Y-S, Jung M-Y, Sarkissian M, Richter JD. 2002. N-methyl-D-aspartate receptor signaling results in Aurora kinase-catalyzed CPEB phosphorylation and alpha CaMKII mRNA polyadenylation at synapses. *EMBO J*. **21**:2139–2148.
- Huang Y-S, Kan M-C, Lin C-L, Richter JD. 2006. CPEB3 And CPEB4 in neurons: analysis of RNA-binding specificity and translational control of AMPA receptor GluR2 mRNA. *EMBO J*. **25**:4865–4876.
- Ivshina M, Lasko P, Richter JD. 2014. Cytoplasmic polyadenylation element binding proteins in development, health, and disease. *Annu Rev Cell Dev Biol*. **30**:393–415.
- Jacobson A. 1996. Poly(A) metabolism and translation: The closed-loop model. In: Hershey JWB, Mathews MB, Sonenberg N, editors. *Translational control*. Cold Spring Harbor Laboratory Press. p. 451–480.
- Jacobson A, Peltz SW. 1996. Interrelationships of the pathways of mRNA decay and translation in eukaryotic cells. *Annu Rev Biochem*. **65**:693–739.
- Kahvejian A, Svitkin YV, Sukarieh R, M'Boutchou MN, Sonenberg N. 2005. Mammalian poly(A)-binding protein is a eukaryotic translation initiation factor, which acts via multiple mechanisms. *Genes Dev*. **19**:104–113.
- Katoh K, Frith MC. 2012. Adding unaligned sequences into an existing alignment using MAFFT and LAST. *Bioinformatics* **28**:3144–3146.
- Keleman K, Kruttner S, Alenius M, Dickson BJ. 2007. Function of the *Drosophila* CPEB protein Orb2 in long-term courtship memory. *Nat Neurosci*. **10**:1587–1593.
- Kessler MM, Henry MF, Shen E, Zhao J, Gross S, Silver PA, Moore CL. 1997. Hrp1, a sequence-specific RNA-binding protein that shuttles between the nucleus and the cytoplasm, is required for mRNA 3'-end formation in yeast. *Genes Dev*. **11**:2545–2556.
- Kozlov E, Shidlovskii YV, Gilmutdinov R, Schedl P, Zhukova M. 2021. The role of CPEB family proteins in the nervous system function in the norm and pathology. *Cell Biosci*. **11**:64.
- Kronja I, Orr-Weaver TL. 2011. Translational regulation of the cell cycle: when, where, how and why? *Philos Trans R Soc Lond B Biol Sci*. **366**:3638–3652.
- Kruttner S, Stepien B, Noordermeer JN, Mommaas MA, Mechtler K, Dickson BJ, Keleman K. 2012. *Drosophila* CPEB Orb2A mediates memory independent of its RNA-binding domain. *Neuron* **76**:383–395.
- Kuhn U, Gundel M, Knoth A, Kerwitz Y, Rudel S, Wahle E. 2009. Poly(A) tail length is controlled by the nuclear poly(A)-binding protein regulating the interaction between poly(A) polymerase and the cleavage and polyadenylation specificity factor. *J Biol Chem*. **284**:22803–22814.
- Kwak JE, Drier E, Barbee SA, Ramaswami M, Yin JC, Wickens M. 2008. GLD2 poly(A) polymerase is required for long-term memory. *Proc Natl Acad Sci U S A*. **105**:14644–14649.
- Kwak JE, Wang L, Ballantyne S, Kimble J, Wickens M. 2004. Mammalian GLD-2 homologs are poly(A) polymerases. *Proc Natl Acad Sci U S A*. **101**:4407–4412.
- Kwak JE, Wickens M. 2007. A family of poly(U) polymerases. *RNA*. **13**:860–867.
- Lang BF, O'Kelly C, Nerad T, Gray MW, Burger G. 2002. The closest unicellular relatives of animals. *Curr Biol*. **12**:1773–1778.
- Lantz V, Chang JS, Horabin JJ, Bopp D, Schedl P. 1994. The *Drosophila* orb RNA-binding protein is required for the formation of the egg chamber and establishment of polarity. *Genes Dev*. **8**:598–613.
- Lasko P. 2009. Translational control during early development. *Prog Mol Biol Transl Sci*. **90**:211–254.
- Layden MJ, Meyer NP, Pang K, Seaver EC, Martindale MQ. 2010. Expression and phylogenetic analysis of the zic gene family in the evolution and development of metazoans. *Evodevo* **1**:12.
- Layden MJ, Rottinger E, Wolenski FS, Gilmore TD, Martindale MQ. 2013. Microinjection of mRNA or morpholinos for reverse genetic analysis in the starlet sea anemone, *Nematostella vectensis*. *Nat Protoc*. **8**:924–934.
- Lima SA, Chipman LB, Nicholson AL, Chen YH, Yee BA, Yeo GW, Collier J, Pasquinelli AE. 2017. Short poly(A) tails are a conserved feature of highly expressed genes. *Nat Struct Mol Biol*. **24**:1057–1063.
- Lim J, Ha M, Chang H, Kwon SC, Simanshu DK, Patel DJ, Kim VN. 2014. Uridylation by TUT4 and TUT7 marks mRNA for degradation. *Cell* **159**:1365–1376.
- Lim J, Kim D, Lee Y-S, Ha M, Lee M, Yeo J, Chang H, Song J, Ahn K, Kim VN. 2018. Mixed tailing by TENT4A and TENT4B shields mRNA from rapid deadenylation. *Science* **361**:701–704.
- Lin CL, Evans V, Shen S, Xing Y, Richter JD. 2010. The nuclear experience of CPEB: implications for RNA processing and translational control. *RNA*. **16**:338–348.
- Lindqvist A, Rodriguez-Bravo V, Medema RH. 2009. The decision to enter mitosis: feedback and redundancy in the mitotic entry network. *J Cell Biol*. **185**:193–202.
- Luitjens C, Gallegos M, Kraemer B, Kimble J, Wickens M. 2000. CPEB proteins control two key steps in spermatogenesis in *C. elegans*. *Genes Dev*. **14**:2596–2609.
- Majumdar A, Cesario WC, White-Grindley E, Jiang H, Ren F, Khan MR, Li L, Choi EM, Kannan K, Guo F, et al. 2012. Critical role of amyloid-like oligomers of *Drosophila* Orb2 in the persistence of memory. *Cell* **148**:515–529.
- Mangus DA, Evans MC, Jacobson A. 2003. Poly(A)-binding proteins: multifunctional scaffolds for the post-transcriptional control of gene expression. *Genome Biol*. **4**:223.
- Mathews M, Sonenberg N, Hershey JWB. 2007. *Translational control in biology and medicine*. Cold Spring Harbor (NY): Cold Spring Harbor Laboratory Press.

- McGrew LL, Richter JD. 1990. Translational control by cytoplasmic polyadenylation during *Xenopus* oocyte maturation: characterization of cis and trans elements and regulation by cyclin/MPP. *EMBO J.* **9**:3743–3751.
- Meaux SA, Holmquist CE, Marzluff WF. 2018. Role of oligouridylation in normal metabolism and regulated degradation of mammalian histone mRNAs. *Philos Trans R Soc Lond B Biol Sci.* **373**:20180170.
- Medina M, Collins AG, Taylor JW, Valentine JW, Lipps JH, Amaral-Zettler L, Sogin ML. 2003. Phylogeny of Opisthokonta and the evolution of multicellularity and complexity in Fungi and Metazoa. *Int J Astrobiol.* **2**:203–211.
- Mendez R, Hake LE, Andresson T, Littlepage LE, Ruderman JV, Richter JD. 2000. Phosphorylation of CPE binding factor by Eg2 regulates translation of c-mos mRNA. *Nature* **404**:302–307.
- Mendez R, Murthy KG, Ryan K, Manley JL, Richter JD. 2000. Phosphorylation of CPEB by Eg2 mediates the recruitment of CPSF into an active cytoplasmic polyadenylation complex. *Mol Cell.* **6**:1253–1259.
- Mendez R, Richter JD. 2001. Translational control by CPEB: a means to the end. *Nat Rev Mol Cell Biol.* **2**:521–529.
- Menichelli E, Wu J, Campbell ZT, Wickens M, Williamson JR. 2013. Biochemical characterization of the *Caenorhabditis elegans* FBF.CPB-1 translational regulation complex identifies conserved protein interaction hotspots. *J Mol Biol.* **425**:725–737.
- Merkel DJ, Wells SB, Hilburn BC, Elazzouzi F, Perez-Alvarado GC, Lee BM. 2013. The C-terminal region of cytoplasmic polyadenylation element binding protein is a ZZ domain with potential for protein–protein interactions. *J Mol Biol.* **425**:2015–2026.
- Minshall N, Reiter MH, Weil D, Standart N. 2007. CPEB interacts with an ovary-specific eIF4E and 4E-T in early *Xenopus* oocytes. *J Biol Chem.* **282**:37389–37401.
- Minvielle-Sebastia L, Beyer K, Krecic AM, Hector RE, Swanson MS, Keller W. 1998. Control of cleavage site selection during mRNA 3' end formation by a yeast hnRNP. *EMBO J.* **17**:7454–7468.
- Mitchell DG, Edgar A, Martindale MQ. 2021. Improved histological fixation of gelatinous marine invertebrates. *Front Zool.* **18**:29.
- Modepalli V, Moran Y. 2017. Evolution of miRNA tailing by 3' terminal uridylyl transferases in metazoa. *Genome Biol Evol.* **9**(6):1547–1560.
- Moreland RT, Nguyen AD, Ryan JF, Baxevasis AD. 2020. The Mnemiopsis Genome Project Portal: integrating new gene expression resources and improving data visualization. *Database (Oxford).* **2020**:baaa029.
- Moreland RT, Nguyen AD, Ryan JF, Schnitzler CE, Koch BJ, Siewert K, Wolfsberg TG, Baxevasis AD. 2014. A customized Web portal for the genome of the ctenophore *Mnemiopsis leidyi*. *BMC Genomics.* **15**:316.
- Morgan DO. 1997. Cyclin-dependent kinases: engines, clocks, and microprocessors. *Annu Rev Cell Dev Biol.* **13**:261–291.
- Morozov IY, Jones MG, Gould PD, Crome V, Wilson JB, Hall AJ, Rigden DJ, Caddick MX. 2012. mRNA 3' tagging is induced by nonsense-mediated decay and promotes ribosome dissociation. *Mol Cell Biol.* **32**:2585–2595.
- Nakahata S, Katsu Y, Mita K, Inoue K, Nagahama Y, Yamashita M. 2001. Biochemical identification of *Xenopus* Pumilio as a sequence-specific cyclin B1 mRNA-binding protein that physically interacts with a nanos homolog, Xcat-2, and a cytoplasmic polyadenylation element-binding protein. *J Biol Chem.* **276**:20945–20953.
- Nguyen L-T, Schmidt HA, von Haeseler A, Minh BQ. 2015. IQ-TREE: a fast and effective stochastic algorithm for estimating maximum-likelihood phylogenies. *Mol Biol Evol.* **32**:268–274.
- Norvell A, Wong J, Randolph K, Thompson L. 2015. Wispy and Orb cooperate in the cytoplasmic polyadenylation of localized gurken mRNA. *Dev Dyn.* **244**:1276–1285.
- Ochi H, Chiba K. 2016. Hormonal stimulation of starfish oocytes induces partial degradation of the 3' termini of cyclin B mRNAs with oligo(U) tails, followed by poly(A) elongation. *RNA.* **22**:822–829.
- Oroz J, Felix SS, Cabrera EJ, Laurents DV. 2020. Structural transitions in Orb2 prion-like domain relevant for functional aggregation in memory consolidation. *J Biol Chem.* **295**:18122–18133.
- Pai T-P, Chen C-C, Lin H-H, Chin A-L, Lai JS-Y, Lee P-T, Chiang A-S. 2013. *Drosophila* ORB protein in two mushroom body output neurons is necessary for long-term memory formation. *Proc Natl Acad Sci U S A.* **110**:7898–7903.
- Pang K, Martindale MQ. 2008. *Mnemiopsis leidyi* spawning and embryo collection. *CSH Protoc.* **2008**:pdb prot5085.
- Paps J, Holland PWH. 2018. Reconstruction of the ancestral metazoan genome reveals an increase in genomic novelty. *Nat Commun.* **9**:1730.
- Park J-E, Yi H, Kim Y, Chang H, Kim VN. 2016. Regulation of poly(A) tail and translation during the somatic cell cycle. *Mol Cell.* **62**:462–471.
- Pique M, Lopez JM, Foissac S, Guigo R, Mendez R. 2008. A combinatorial code for CPE-mediated translational control. *Cell* **132**:434–448.
- Potter SC, Luciani A, Eddy SR, Park Y, Lopez R, Finn RD. 2018. HMMER web server: 2018 update. *Nucleic Acids Res.* **46**:W200–W204.
- Preston MA, Porter DF, Chen F, Buter N, Lapointe CP, Keles S, Kimble J, Wickens M. 2019. Unbiased screen of RNA tailing activities reveals a poly(UG) polymerase. *Nat Methods.* **16**:437–445.
- Puoti A, Gallegos M, Zhang B, Wickens MP, Kimble J. 1997. Controls of cell fate and pattern by 3' untranslated regions: the *Caenorhabditis elegans* sperm/oocyte decision. *Cold Spring Harb Symp Quant Biol.* **62**:19–24.
- Putnam NH, Srivastava M, Hellsten U, Dirks B, Chapman J, Salamov A, Terry A, Shapiro H, Lindquist E, Kapitonov VV, et al. 2007. Sea anemone genome reveals ancestral eumetazoan gene repertoire and genomic organization. *Science* **317**:86–94.
- Quail MA, Smith M, Coupland P, Otto TD, Harris SR, Connor TR, Bertoni A, Swerdlow HP, Gu Y. 2012. A tale of three next generation sequencing platforms: comparison of Ion Torrent, Pacific Biosciences and Illumina MiSeq sequencers. *BMC Genomics.* **13**:341.
- Racki WJ, Richter JD. 2006. CPEB controls oocyte growth and follicle development in the mouse. *Development* **133**:4527–4537.
- Radford HE, Meijer HA, de Moor CH. 2008. Translational control by cytoplasmic polyadenylation in *Xenopus* oocytes. *Biochim Biophys Acta.* **1779**:217–229.
- Ramon-Mateu J, Edgar A, Mitchell D, Martindale MQ. 2022. Studying Ctenophora WBR using *Mnemiopsis leidyi*. *Methods Mol Biol.* **2450**:95–119.
- Rassa JC, Wilson GM, Brewer GA, Parks GD. 2000. Spacing constraints on reinstitution of paramyxovirus transcription: the gene end U tract acts as a spacer to separate gene end from gene start sites. *Virology* **274**:438–449.
- Raveendra BL, Siemer AB, Puthanveetil SV, Hendrickson WA, Kandel ER, McDermott AE. 2013. Characterization of prion-like conformational changes of the neuronal isoform of *Aplysia* CPEB. *Nat Struct Mol Biol.* **20**:495–501.
- Richter JD. 1999. Cytoplasmic polyadenylation in development and beyond. *Microbiol Mol Biol Rev.* **63**:446–456.
- Richter JD, Lasko P. 2011. Translational control in oocyte development. *Cold Spring Harb Perspect Biol.* **3**:a002758.
- Rosenthal ET, Hunt T, Ruderman JV. 1980. Selective translation of mRNA controls the pattern of protein synthesis during early development of the surf clam, *Spisula solidissima*. *Cell* **20**:487–494.
- Rouhana L, Tasaki J, Saberi A, Newmark PA. 2017. Genetic dissection of the planarian reproductive system through characterization of *Schmidtea mediterranea* CPEB homologs. *Dev Biol.* **426**:43–55.
- Rouhana L, Wang L, Buter N, Kwak JE, Schiltz CA, Gonzalez T, Kelley AE, Landry CF, Wickens M. 2005. Vertebrate GLD2 poly(A) polymerases in the germline and the brain. *RNA.* **11**:1117–1130.
- Rouhana L, Wickens M. 2007. Autoregulation of GLD-2 cytoplasmic poly(A) polymerase. *RNA.* **13**:188–199.

- Roy B, Jacobson A. 2013. The intimate relationships of mRNA decay and translation. *Trends Genet.* **29**:691–699.
- Rozanski A, Moon H, Brandl H, Martin-Duran JM, Grohme MA, Huttner K, Bartscherer K, Henry I, Rink JC. 2019. Planmine 3.0-improvements to a mineable resource of flatworm biology and biodiversity. *Nucleic Acids Res.* **47**:D812–D820.
- Rutledge CE, Lau HT, Mangan H, Hardy LL, Sunnotel O, Guo F, MacNicol AM, Walsh CP, Lees-Murdock DJ. 2014. Efficient translation of Dnmt1 requires cytoplasmic polyadenylation and Musashi binding elements. *PLoS One.* **9**:e88385.
- Ryan JF, Pang K, Schnitzler CE, Nguyen AD, Moreland RT, Simmons DK, Koch BJ, Francis WR, Havlak P, Program NCS, et al. 2013. The genome of the ctenophore *Mnemiopsis leidyi* and its implications for cell type evolution. *Science* **342**:1242592.
- Sachs AB, Bond MW, Kornberg RD. 1986. A single gene from yeast for both nuclear and cytoplasmic polyadenylate-binding proteins: domain structure and expression. *Cell* **45**:827–835.
- Sachs AB, Varani G. 2000. Eukaryotic translation initiation: there are (at least) two sides to every story. *Nat Struct Biol.* **7**:356–361.
- Salles FJ, Lieberfarb ME, Wreden C, Gergen JP, Strickland S. 1994. Coordinate initiation of *Drosophila* development by regulated polyadenylation of maternal messenger RNAs. *Science* **266**:1996–1999.
- Sartain CV, Cui J, Meisel RP, Wolfner MF. 2011. The poly(A) polymerase GLD2 is required for spermatogenesis in *Drosophila melanogaster*. *Development* **138**:1619–1629.
- Sasson DA, Ryan JF. 2016. The sex lives of ctenophores: the influence of light, body size, and self-fertilization on the reproductive output of the sea walnut, *Mnemiopsis leidyi*. *PeerJ.* **4**:e1846.
- Schultz DT, Francis WR, McBroome JD, Christianson LM, Haddock SHD, Green RE. 2021. A chromosome-scale genome assembly and karyotype of the ctenophore *Hormiphora californensis*. *G3 (Bethesda)*. **11**:jkab302.
- Sement FM, Ferrier E, Zuber H, Merret R, Alioua M, Deragon JM, Bousquet-Antonelli C, Lange H, Gagliardi D. 2013. Uridylation prevents 3' trimming of oligoadenylated mRNAs. *Nucleic Acids Res.* **41**:7115–7127.
- Setoyama D, Yamashita M, Sagata N. 2007. Mechanism of degradation of CPEB during *Xenopus* oocyte maturation. *Proc Natl Acad Sci U S A.* **104**:18001–18006.
- Sheets MD. 2019. Assaying NanoLuc luciferase activity from mRNA-injected *Xenopus* embryos. *Methods Mol Biol.* **1920**:33–39.
- Sheets MD, Fox CA, Hunt T, Vande Woude G, Wickens M. 1994. The 3'-untranslated regions of *c-mos* and cyclin mRNAs stimulate translation by regulating cytoplasmic polyadenylation. *Genes Dev.* **8**:926–938.
- Shen B, Goodman HM. 2004. Uridine addition after microRNA-directed cleavage. *Science* **306**:997.
- Shukla A, Yan J, Pagano DJ, Dodson AE, Fei Y, Gorham J, Seidman JG, Wickens M, Kennedy S. 2020. Poly(UG)-tailed RNAs in genome protection and epigenetic inheritance. *Nature* **582**:283–288.
- Si K, Giustetto M, Etkin A, Hsu R, Janisiewicz AM, Miniaci MC, Kim JH, Zhu H, Kandel ER. 2003. A neuronal isoform of CPEB regulates local protein synthesis and stabilizes synapse-specific long-term facilitation in aplysia. *Cell* **115**:893–904.
- Si K, Kandel ER. 2016. The role of functional prion-like proteins in the persistence of memory. *Cold Spring Harb Perspect Biol.* **8**:a021774.
- Si K, Lindquist S, Kandel ER. 2003. A neuronal isoform of the aplysia CPEB has prion-like properties. *Cell* **115**:879–891.
- Simmons DK, Pang K, Martindale MQ. 2012. Lim homeobox genes in the Ctenophore *Mnemiopsis leidyi*: the evolution of neural cell type specification. *Evodevo* **3**:2.
- Sousa Martins JP, Liu X, Oke A, Arora R, Franciosi F, Viville S, Laird DJ, Fung JC, Conti M. 2016. DAZL and CPEB1 regulate mRNA translation synergistically during oocyte maturation. *J Cell Sci.* **129**:1271–1282.
- Stebbins-Boaz B, Hake LE, Richter JD. 1996. CPEB controls the cytoplasmic polyadenylation of cyclin, Cdk2 and *c-mos* mRNAs and is necessary for oocyte maturation in *Xenopus*. *EMBO J.* **15**:2582–2592.
- Stepien BK, Oppitz C, Gerlach D, Dag U, Novatchkova M, Kruttner S, Stark A, Keleman K. 2016. RNA-binding profiles of *Drosophila* CPEB proteins Orb and Orb2. *Proc Natl Acad Sci U S A.* **113**:E7030–E7038.
- Subtelny AO, Eichhorn SW, Chen GR, Sive H, Bartel DP. 2014. Poly(A)-tail profiling reveals an embryonic switch in translational control. *Nature* **508**:66–71.
- Tajrishi MM, Tuteja R, Tuteja N. 2011. Nucleolin: the most abundant multifunctional phosphoprotein of nucleolus. *Commun Integr Biol.* **4**:267–275.
- Tay J, Hodgman R, Richter JD. 2000. The control of cyclin B1 mRNA translation during mouse oocyte maturation. *Dev Biol.* **221**:1–9.
- Udagawa T, Swanger SA, Takeuchi K, Kim JH, Nalavadi V, Shin J, Lorenz LJ, Zukin RS, Bassell GJ, Richter JD. 2012. Bidirectional control of mRNA translation and synaptic plasticity by the cytoplasmic polyadenylation complex. *Mol Cell.* **47**:253–266.
- Vassalli JD, Huarte J, Belin D, Gubler P, Vassalli A, O'Connell ML, Parton LA, Rickles RJ, Strickland S. 1989. Regulated polyadenylation controls mRNA translation during meiotic maturation of mouse oocytes. *Genes Dev.* **3**:2163–2171.
- Vassalli JD, Stutz A. 1995. Translational control. Awakening dormant mRNAs. *Curr Biol.* **5**:476–479.
- Villalba A, Coll O, Gebauer F. 2011. Cytoplasmic polyadenylation and translational control. *Curr Opin Genet Dev.* **21**:452–457.
- Walser CB, Lipshitz HD. 2011. Transcript clearance during the maternal-to-zygotic transition. *Curr Opin Genet Dev.* **21**:431–443.
- Wang L, Eckmann CR, Kadyk LC, Wickens M, Kimble J. 2002. A regulatory cytoplasmic poly(A) polymerase in *Caenorhabditis elegans*. *Nature* **419**:312–316.
- Weill L, Belloc E, Bava FA, Mendez R. 2012. Translational control by changes in poly(A) tail length: recycling mRNAs. *Nat Struct Mol Biol.* **19**:577–585.
- Weill L, Belloc E, Castellazzi CL, Mendez R. 2017. Musashi 1 regulates the timing and extent of meiotic mRNA translational activation by promoting the use of specific CPEs. *Nat Struct Mol Biol.* **24**:672–681.
- Wickens M. 1990. In the beginning is the end: regulation of poly(A) addition and removal during early development. *Trends Biochem Sci.* **15**:320–324.
- Wickens M, Anderson P, Jackson RJ. 1997. Life and death in the cytoplasm: messages from the 3' end. *Curr Opin Genet Dev.* **7**:220–232.
- Wigington CP, Williams KR, Meers MP, Bassell GJ, Corbett AH. 2014. Poly(A) RNA-binding proteins and polyadenosine RNA: new members and novel functions. *Wiley Interdiscip Rev RNA.* **5**:601–622.
- Wijesena N, Simmons DK, Martindale MQ. 2017. Antagonistic BMP-cWNT signaling in the cnidarian *Nematostella vectensis* reveals insight into the evolution of mesoderm. *Proc Natl Acad Sci U S A.* **114**:E5608–E5615.
- Wilt FH. 1973. Polyadenylation of maternal RNA of sea urchin eggs after fertilization. *Proc Natl Acad Sci U S A.* **70**:2345–2349.
- Xiang K, Bartel DP. 2021. The molecular basis of coupling between poly(A)-tail length and translational efficiency. *Elife.* **10**:e66493.
- Xu S, Hafer N, Agunwamba B, Schedl P. 2012. The CPEB protein Orb2 has multiple functions during spermatogenesis in *Drosophila melanogaster*. *PLoS Genet.* **8**:e1003079.
- Yu S, Kim VN. 2020. A tale of non-canonical tails: gene regulation by post-transcriptional RNA tailing. *Nat Rev Mol Cell Biol.* **21**:542–556.
- Zheng D, Tian B. 2014. Sizing up the poly(A) tail: insights from deep sequencing. *Trends Biochem Sci.* **39**:255–257.
- Zimmermann B, Robb SMC, Genikhovich G, Fropp WJ, Weilguny L, He S, Chen S, Lovegrove-Walsh J, Hill EM, Chen C-Y, et al. 2022. Sea anemone genomes reveal ancestral metazoan chromosomal macrosynteny. *bioRxiv:2020.2010.2030.359448*. doi:10.1101/2020.10.30.359448